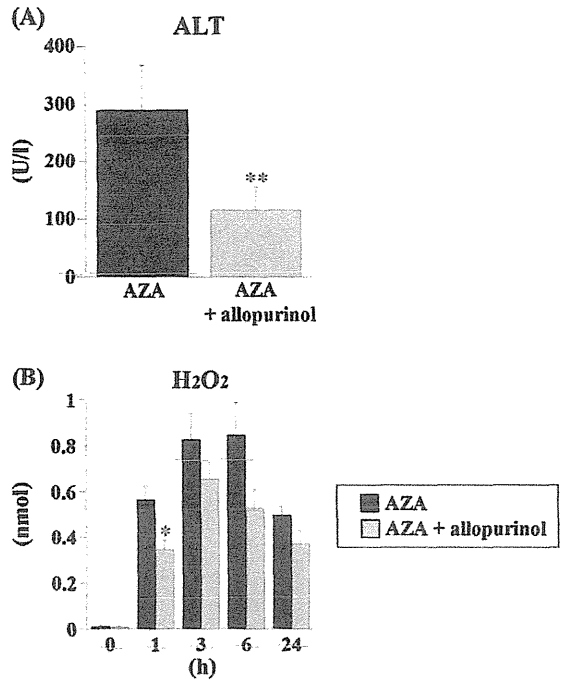

Fig. 3. Effect of a xanthine oxidase inhibitor on the plasma ALT levels and time-dependent changes in the plasma H_2O_2 levels in mice with AZA-induced liver injury. (A) The mice were administered AZA (200 mg/kg in corn oil, *p.o.*) and allopurinol (30 mg/kg in sterilize PBS, *i.p.*) simultaneously for three days. The plasma ALT levels were measured 24 h after the last administration. (B) The plasma H_2O_2 levels were measured 1, 3, 6, and 24 h after the last administration. The data represent the mean ± SEM ($n = 4$–5). *,**Significantly different compared with AZA-treated mice ($^*p < 0.05$, $^{**}p < 0.01$).

AZA-induced liver injury (Jeurissen et al., 1990). Although this observation suggests that immunological mechanisms underlie the pathogenesis of AZA-induced liver injury, the involvement of immune- and inflammation-related factors in AZA-induced liver injury *in vivo* has never been reported. In this study, we established a mouse model of AZA-induced liver injury and investigated the involvement of both oxidative stress and immunological responses in AZA-induced liver injury.

First, we investigated the effect of different AZA dosing program. Because AZA is administered orally in clinical practice, we administered AZA orally to mice. The dose of 200 mg/kg (*p.o.*, approximately one-twelfth of the murine oral LD50) was adopted, and the plasma ALT levels were measured 24 h after the last AZA administration, which is the time point that showed the highest ALT levels (Fig. 1B and C). Using the selected dosing program, the ALT and AST levels started to increase on day 3 and were markedly higher on days 5 and 6 (Fig. 1A). Furthermore, liver injury was confirmed through the histological evaluation of liver sections obtained from mice six days after the last AZA administration (Fig. 1D). We regarded the increase in the plasma ALT levels on day 3 as the initiation phase of AZA-induced liver injury and the higher increases on days 5 and 6 as the exacerbation phase. Clinical reports have shown that acute and chronic liver injury develops within weeks-years and 1–5 years after the initiation of AZA treatment, respectively. Liver injury has been recognized in 2% of AZA-treated patients. To definitely induce liver injury, we administered an AZA dose that was 40-fold higher than the clinical dose.

Hepatic GSH is consumed during the metabolism of AZA into 6-MP catalyzed by glutathione S-transferases. GSH is responsible for ROS scavenging and is converted into GSSG. Therefore, the decrease in GSH and the increase in GSSG induced by AZA administration may be caused by the AZA metabolism and ROS scavenging (Fig. 2A). The low GSH/GSSG ratio suggests that the AZA-treated mice are vulnerable to oxidative stress. The increase of hepatic protein carbonyl levels (Fig. 2B), the decrease of hepatic SOD activities (Fig. 2C), and the suppression of the increased plasma ALT levels by the antioxidant tempol (Fig. 2D) in AZA-treated mice indicate the involvement of oxidative stress in AZA-induced liver injury *in vivo* in mice. The decreased SOD activities in the AZA-treated mice were recovered by tempol administration (Fig. 2E), which suggests that tempol ameliorates the AZA-induced liver injury through the suppression of oxidative stress. It is interesting to note that GSH/GSSG ratio was decreased by AZA treatment from day 1, when ALT level was not changed. In addition, content of hepatic protein carbonyl and SOD activities showed the increasing and the decreasing tendency, respectively from day 3. These results suggested that the oxidative stress is involved in AZA-induced liver injury from early stage.

The metabolic conversion of 6-MP into 6-thiouric acid *via* XO, which is a critical source of ROS, potentially leads to hepatotoxicity. We inhibited XO using allopurinol, which is an inhibitor of XO, to investigate the involvement of XO in AZA-induced liver injury. The increased plasma ALT levels in AZA-treated mice were suppressed by allopurinol (Fig. 3A). An allopurinol dose of 30 mg/kg was sufficient to inhibit the XO activity in mice, as reported previously (Zhao et al., 2006). To investigate whether ROS was decreased by allopurinol, the plasma H_2O_2 levels were measured on day 3. The results show that allopurinol suppressed the plasma H_2O_2 levels (Fig. 3B). Although a significant change was recognized only 1 h after the last AZA administration, the plasma H_2O_2 levels in the allopurinol-treated mice tended to decrease over a period of 24 h. These data suggest that XO-induced ROS are involved in AZA-induced liver injury in mice. However, this effect of allopurinol was not observed on days 5 and 6 (data not shown), which suggests that the ROS generation through the AZA metabolism may be involved only in the initiation phase of liver injury.

It has been reported that ROS induces the expression of TLR4 ligands and RAGE (Yao and Brownlee, 2010). We thus investigated whether these factors are involved in AZA-induced liver injury. The hepatic mRNA levels and the plasma protein levels of receptors (TLR2, TLR4, and RAGE) and their ligands (S100A8, S100A9, and HMGB1) were significantly increased in AZA-induced liver injury (Fig. 4A and B), particularly during the late phase (on days 5 and 6). Therefore, we administered eritoran, a TLR4 antagonist, to mice on day 5 of AZA administration. The protective effect of eritoran for DILI was previously investigated in detail and was reported in carbamazepine-induced liver injury in mice (Higuchi et al., 2012b). In this study, we adapted the same dosing and timing schedule in AZA administration. A significant decrease in the plasma ALT levels was found in the AZA plus eritoran-treated mice compared with the AZA-treated mice (Fig. 4C), which indicates that the activation of the innate immune system contributes to the exacerbation phase of AZA-induced liver injury. However, the protective effect was relatively modest, which suggested the TLR4 signaling was partly involved in AZA-induced liver injury.

The hepatic mRNA levels of T cell-related factors were not significantly changed by AZA administration (Fig. 5A). The expression level of T-bet, which is a transcription factor of Th1 cells, was significantly increased on day 5. However, the expression level of IFN-γ, a pro-inflammatory cytokine secreted by Th1 cells, was not changed. In addition, changes in the plasma protein levels of IL-4 and IL-17, which are pro-inflammatory cytokines secreted by Th2 and Th17 cells, respectively, were not detected (data not shown). These results suggest that the pharmacological effect of AZA, *i.e.*, immune suppression, might inhibit the response of T cells. Thus, these T cell-related factors are not likely to be involved in AZA-induced liver injury.

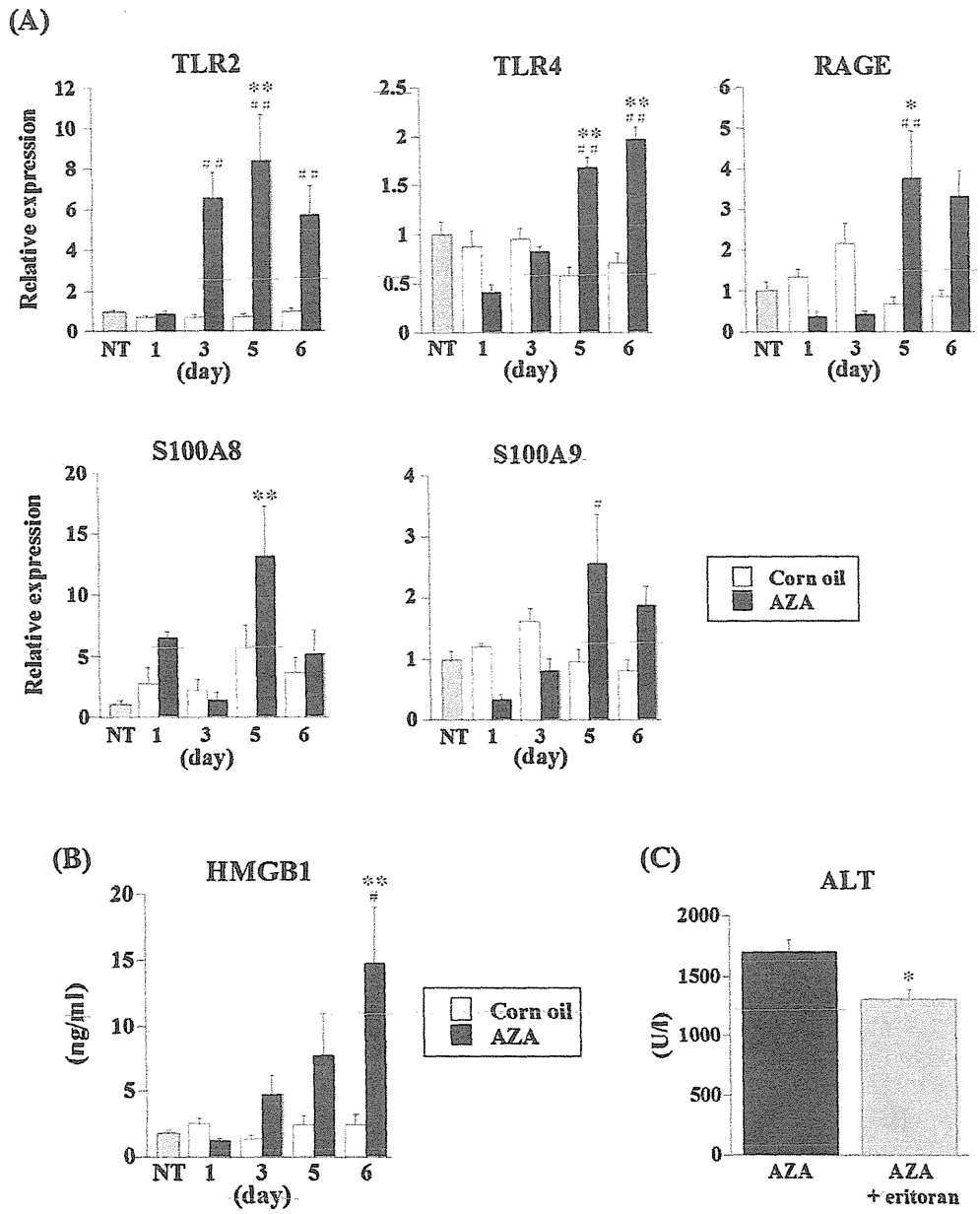

Fig. 4. Time-dependent changes in the hepatic mRNA expression levels of DAMP-related genes and the plasma HMGB1 protein levels and effect of a TLR4 antagonist on the plasma ALT levels in mice with AZA-induced liver injury. (A and B) The mice were administered AZA (200 mg/kg in corn oil, *p.o.*) once daily for six days. Mice that were orally administered corn oil were used as the control. The hepatic mRNA expression levels of DAPM-related genes and the plasma HMGB1 protein levels were measured 24 h after AZA was administered for one, three, five, and six days. The data represent the mean ± SEM ($n = 4$–6). *,**,#,##Significantly different compared with non-treated (NT) mice (*$p < 0.05$, **$p < 0.01$) and corn oil-treated mice (#$p < 0.05$, ##$p < 0.01$). (C) The mice were administered AZA (200 mg/kg in corn oil, *p.o.*) once daily for five days, and eritoran (50 μg/mouse in 0.2 ml sterile saline, *i.v.*) was administered with the last AZA administration (on day 5). The plasma ALT levels were measured 24 h after the last administration. The data represent the mean ± SEM ($n = 4$–6). *Significantly different compared with AZA-treated mice (*$p < 0.05$).

By contrast, the hepatic mRNA levels of inflammation-related factors (TNF-α, IL-1β, MIP-2, and NALP3) were significantly increased in the AZA-treated mice (Fig. 5A). TNF-α and IL-1β are pro-inflammatory cytokines produced by a variety of immune cells, such as macrophages, mast cells, and dendritic cells (Tracey, 1994; Arend et al., 2008). MIP-2 is a chemokine released by macrophages. IL-1β and MIP-2 recruit leukocytes, particularly neutrophils, into the liver (Bajt et al., 2001). The NALP3 inflammasome mediates the processing of IL-1β, which is activated by ROS and DAMPs (Agostini et al., 2004). The infiltration of neutrophils was confirmed by anti-MPO straining (Fig. 5B). These data suggest the involvement of the inflammatory response in the exacerbation phase of AZA-induced liver injury.

Based on the presented data, AZA-induced liver injury might be caused by oxidative stress through the generation of ROS during the initiation phase of hepatotoxicity. In contrast, inflammation-related factors might be involved in the exacerbation phase. In other words, the injury of hepatocytes by oxidative stress might be the first step of AZA-induced liver injury, and this step is likely followed by the inflammatory response induced by the DAMPs released by necrotic hepatocytes. The putative mechanism of AZA-induced liver injury is summarized in Fig. 6.

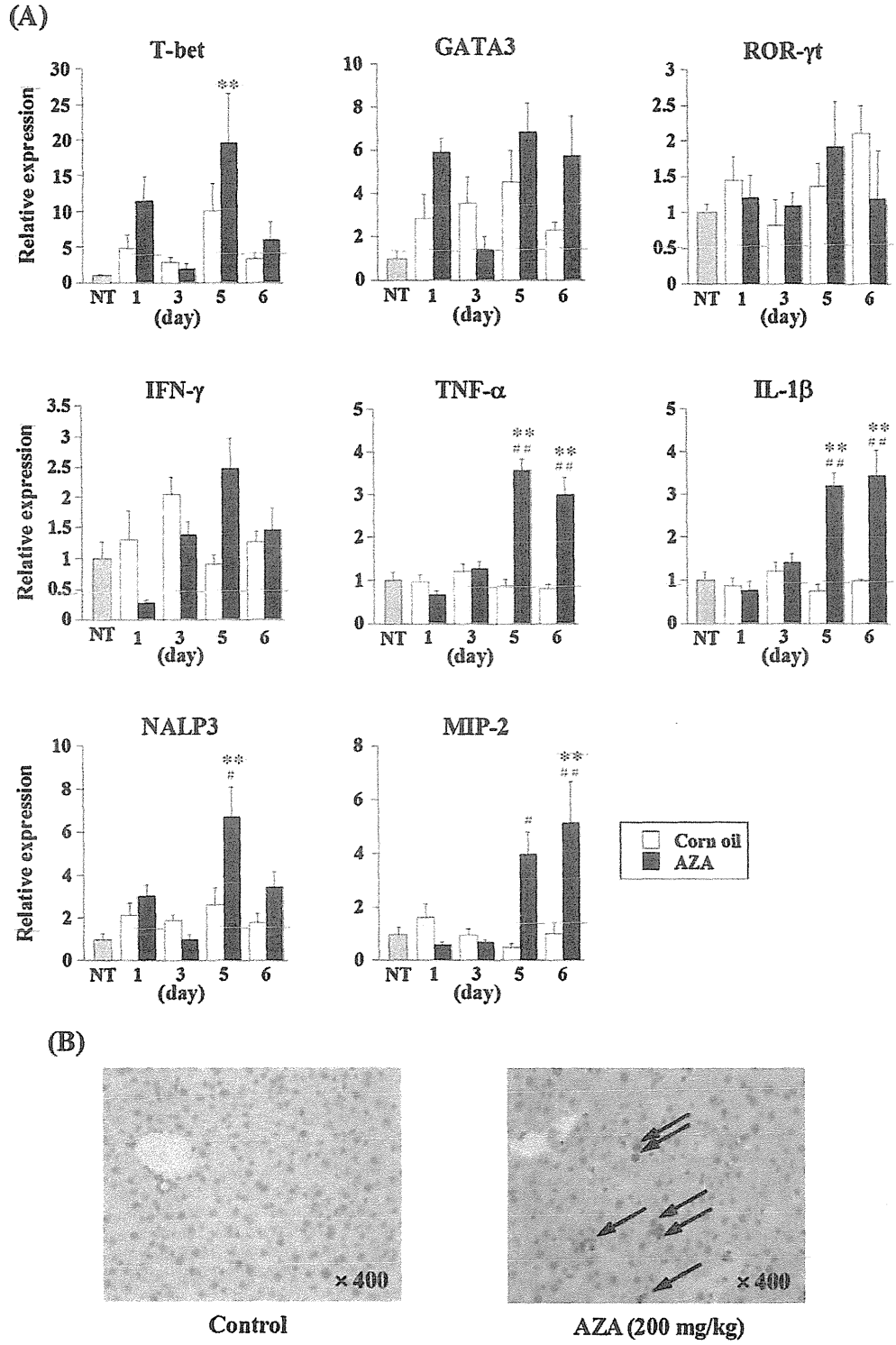

Fig. 5. Time-dependent changes in the hepatic mRNA expression levels of T-cell transcription factors and inflammation-related factors. (A) AZA was administered using the dosing schedule described in Fig. 4. (A and B) The data represent the mean ± SEM ($n = 4$–6). *,**,#,##Significantly different compared with non-treated (NT) mice (*$p < 0.05$, **$p < 0.01$) and corn oil-treated mice (#$p < 0.05$, ##$p < 0.01$). (B) The mononuclear cell infiltration was assessed by immunostaining for MPO. The black arrows indicate MPO-positive cells.

It is hypothesized that multiple mechanisms cause AZA-induced liver injury. A case study suggested the contribution of genetic factors because two of three patients who developed AZA-induced liver injury possessed similar HLA haplotypes (Jeurissen et al., 1990). Alternatively, TPMT is an enzyme that mediates the methylation of 6-MP. High TPMT activity and methylated metabolites levels have been correlated with hepatotoxicity in humans (Dubinsky et al., 2002; Van Asseldonk et al., 2012), which suggests that reactive metabolites may be involved in AZA-induced liver injury. These factors should be considered in future studies.

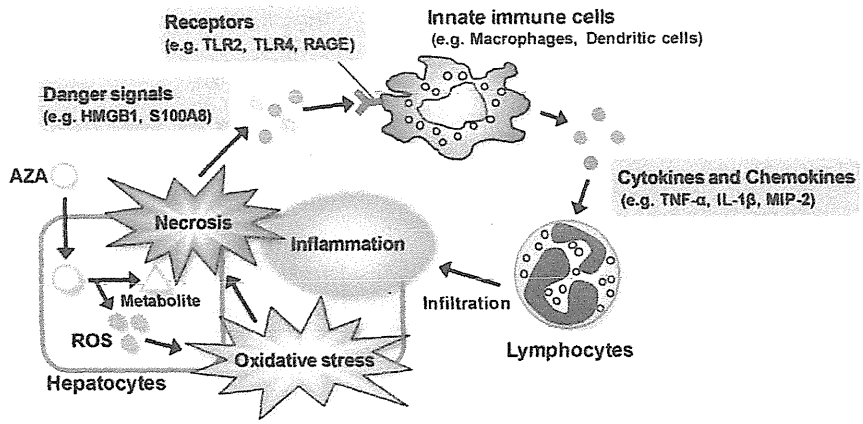

Fig. 6. The putative mechanism of AZA-induced liver injury. During metabolism of AZA in hepatocytes, ROS are produced. ROS-induced oxidative stress causes necrosis of hepatocytes. Danger signals released from hepatocytes activate innate immune cells *via* their receptors. Activated innate immune cells lead to the secretion of cytokines and chemokines, which resulted in inflammation in the liver.

to further clarify the mechanism of AZA-induced liver injury in humans.

In conclusion, we successfully established a mouse model of AZA-induced liver injury and demonstrated the involvement of oxidative stress, the generation of ROS, and inflammation-related factors in AZA-induced liver injury. Based on our findings, inflammation-related factors are associated with the exacerbation phase of AZA-induced liver injury. In contrast, oxidative stress and ROS generation may affect the initiation phase of AZA-induced liver injury. Furthermore, we showed the potential effectiveness of allopurinol, antioxidant agents, and TLR4 inhibitors for the treatment of AZA-induced liver injury. These finding may provide insight into the mechanisms of DILI.

Funding

This study was funded by Health and Labor Sciences Research Grants from the Ministry of Health, Labor, and Welfare of Japan (H23-BIO-G001).

Conflict of interest

None of the authors have any conflicts of interest related to this manuscript.

References

Agarwal, R., MacMillan-Crow, L.A., Rafferty, T.M., Saba, H., Roberts, D.W., Fifer, E.K., James, L.P., Hinson, J.A., 2011. Acetaminophen-induced hepatotoxicity in mice occurs with inhibition of activity and nitration of mitochondrial manganese superoxide dismutase. J. Pharmacol. Exp. Ther. 337, 110–116.

Agostini, L., Martinon, F., Burns, K., McDermott, M.F., Hawkins, P.N., Tschopp, J., 2004. NALP3 forms an IL-1β-processing inflammasome with increased activity in Muckle-Wells autoinflammatory disorder. Immunity 20, 319–325.

Aithal, G.P., 2011. Hepatotoxicity related to antirheumatic drugs. Nat. Rev. Rheumatol. 7, 139–150.

Amin, A., Hamza, A.A., 2005. Hepatoprotective effects of Hibiscus, Rosmarinus and Salvia on azathioprine-induced toxicity in rats. Life Sci. 77, 266–278.

Ansari, A., Elliott, T., Baburajan, B., Mayhead, P., O'Donohue, J., Chocair, P., Sanderson, J., Duley, J., 2008. Long-term outcome of using allopurinol co-therapy as a strategy for overcoming thiopurine hepatotoxicity in treating inflammatory bowel disease. Aliment. Pharmacol. Ther. 28, 734–741.

Antoine, D.J., Williams, D.P., Kipar, A., Jenkins, R.E., Regan, S.L., Sathish, J.G., Kitteringham, N.R., Park, B.K., 2009. High-mobility group box-1 protein and keratin-18, circulating serum proteins informative of acetaminophen-induced necrosis and apoptosis in vivo. Toxicol. Sci. 112, 521–531.

Arend, W.P., Palmer, G., Gabay, C., 2008. IL-1, IL-18, and IL-33 families of cytokines. Immunol. Rev. 223, 20–38.

Bajt, M.L., Farhood, A., Jaeschke, H., 2001. Effects of CXC chemokines on neutrophil activation and sequestration in hepatic vasculature. Am. J. Physiol. Gastrointest. Liver Physiol. 281, G1188–G1195.

Dejaco, C., Mittermaier, C., Reinisch, W., Gasche, C., Waldhoer, T., Strohmer, H., Moser, G., 2003. Azathioprine treatment and male fertility in inflammatory bowel disease. Gastroenterology 121, 1048–1053.

Dubinsky, M.C., 2004. Azathioprine, 6-mercaptopurine in inflammatory bowel disease: pharmacology, efficacy and safety. Clin. Gastroenterol. Hepatol. 2, 731–743.

Dubinsky, M.C., Yang, H., Hassard, P.V., Seidman, E.G., Kam, L.Y., Abreu, M.T., Targan, S.R., Vasiliauskas, E.A., 2002. 6-MP metabolite profiles provide a biochemical explanation for 6-MP resistance in patients with inflammatory bowel disease. Gastroenterology 122, 904–915.

El-Beshbishy, H.A., Tork, O.M., El-Bab, M.F., Autifi, M.A., 2011. Antioxidant and anti-apoptotic effects of green tea polyphenols against azathioprine-induced liver injury in rats. Pathophysiology 18, 125–135.

Fridovich, I., 1989. Superoxide dismutases. An adaptation to a paramagnetic gas. J. Biol. Chem. 264, 7761–7764.

Hennessy, E.J., Parker, A.E., O'Neill, L.A., 2010. Targeting Toll-like receptors: emerging therapeutics. Nat. Rev. Drug. Discov. 9, 293–307.

Higuchi, S., Kobayashi, M., Yano, A., Tsuneyama, K., Fukami, T., Nakajima, M., Yokoi, T., 2012a. Involvement of Th2 cytokines in the mouse model of flutamide-induced acute liver injury. J. Appl. Toxicol. 32, 815–822.

Higuchi, S., Kobayashi, M., Yoshikawa, Y., Tsuneyama, K., Fukami, T., Nakajima, M., Yokoi, T., 2011. IL-4 mediates dicloxacillin-induced liver injury in mice. Toxicol. Lett. 200, 139–145.

Higuchi, S., Yano, A., Takai, S., Tsuneyama, K., Fukami, T., Nakajima, M., Yokoi, T., 2012b. Metabolic activation and inflammation reactions involved in carbamazepine-induced liver injury. Toxicol. Sci. 130, 4–16.

Hisamuddin, I.M., Wehbi, M.A., Yang, V.W., 2007. Pharmacogenetics and diseases of the colon. Curr. Opin. Gastroenterol. 23, 60–66.

Holt, M.P., Ju, C., 2006. Mechanisms of drug-induced liver injury. AAPS J. 8, 48–54.

Jeurissen, M.E., Boerbooms, A.M., van de Putte, L.B., Kruijsen, M.W., 1990. Azathioprine induced fever, chills, rash, and hepatotoxicity in rheumatoid arthritis. Ann. Rheum. Dis. 49, 25–27.

Kidd, P., 2003. Th1/Th2 balance: the hypothesis, its limitations, and implications for health and disease. Altern. Med. Rev. 8, 223–246.

Kita, H., Mackay, I.R., Van De Water, J., Gershwin, M.E., 2001. The lymphoid liver: considerations on pathways to autoimmune injury. Gastroenterology 120, 1485–1501.

Kobayashi, E., Kobayashi, M., Tsuneyama, K., Fukami, T., Nakajima, M., Yokoi, T., 2009. Halothane-induced liver injury is mediated by interleukin-17 in mice. Toxicol. Sci. 111, 302–310.

Kobayashi, M., Higuchi, S., Ide, M., Nishikawa, S., Fukami, T., Nakajima, M., Yokoi, T., 2012. Th2 cytokine-mediated methimazole-induced acute liver injury in mice. J. Appl. Toxicol. 32, 823–833.

Kobayashi, M., Higuchi, S., Mizuno, K., Tsuneyama, K., Fukami, T., Nakajima, M., Yokoi, T., 2010. Interleukin-17 is involved in α-naphthylisothiocyanate-induced liver injury in mice. Toxicology 275, 50–57.

Kumada, T., Tsuneyama, K., Hatta, H., Ishizawa, S., Takano, Y., 2004. Improved 1-h rapid immunostaining method using intermittent microwave irradiation: practicability based on 5 years application in Toyama Medical and Pharmaceutical University Hospital. Mod. Pathol. 17, 1141–1149.

Lotze, M.T., Zeh, H.J., Rubartelli, A., Sparvero, L.J., Amoscato, A.A., Washburn, N.R., Devera, M.E., Liang, X., Tor, M., Billiar, T., 2007. The grateful dead: damage-associated molecular pattern molecules and reduction/oxidation regulate immunity. Immunol. Rev. 220, 60–81.

Maltzman, J., Koretzky, G., 2003. Azathioprine: old drug new actions. J. Clin. Invest. 111, 1122–1124.

Marinaki, A.M., Ansari, A., Duley, J.A., Arenas, M., Sumi, S., Lewis, C.M., Shobowale-Bakre, el-M., Escuredo, E., Fairbanks, L.D., Sanderson, J.D., 2004. Adverse drug

reactions to azathioprine therapy are associated with polymorphism in the gene encoding inosine triphosphate pyrophosphatase (ITPase). Pharmacogenetics 14, 181–187.

Oo, Y.H., Adams, D.H., 2010. The role of chemokines in the recruitment of lymphocytes to the liver. J. Autoimmun. 34, 45–54.

Petit, E., Langouet, S., Akhdar, H., Nicolas-Nicolaz, C., Guillouzo, A., Morel, F., 2008. Differential toxic effects of azathioprine, 6-mercaptopurine and 6-thioguanine on human hepatocytes. Toxicol. In Vitro 22, 632–642.

Savov, J.D., Brass, D.M., Lawson, B.L., McElvania-Tekippe, E., Walker, J.K., Schwartz, D.A., 2005. Toll-like receptor 4 antagonist (E5564) prevents the chronic airway response to inhaled lipopolysaccharide. Am. J. Physiol. Lung Cell Mol. Physiol. 289, L329–L337.

Steinman, L., 2007. A brief history of Th17, the first major revision in the Th1/Th2 hypothesis if T cell-mediated tissue damage. Nat. Rev. Med. 13, 139–145.

Takatsu, N., Matsui, T., Murakami, Y., Ishihara, H., Hisabe, T., Nagahama, T., Maki, S., Beppu, T., Takaki, Y., Hirai, F., Yao, K., 2009. Adverse reactions to azathioprine cannot be predicted by thiopurine S-methyltransferase genotype in Japanese patients with inflammatory bowel disease. J. Gastroenterol. Hepatol. 24, 1258–1264.

Thornalley, P.J., 1998. Cell activation by glycated proteins. AGE receptors, receptor recognition factors and functional classification of AGEs. Cell. Mol. Biol. 44, 1013–1023.

Tietze, F., 1969. Enzymatic method for quantitative determination of nanogram amounts of total and oxidized glutathione: applications to mammalian blood and other tissues. Anal. Biochem. 27, 502–522.

Tracey, K.J., 1994. Tumor necrosis factor-α. In: Thomson, A. (Ed.), The Cytokine Handbook. Academic Press, London, pp. 289–304.

Van Asseldonk, D.P., Seinen, M.L., De Boer, N.K., Van Bodegraven, A.A., Mulder, C.J., 2012. Hepatotoxicity associated with 6-methyl mercaptopurine formation during azathioprine and 6-mercaptopurine therapy does not occur on the short-term during 6-thioguanine therapy in IBD treatment. J. Crohns Colitis 6, 95–101.

Wang, H., Yang, H., Tracey, K.J., 2004. Extracellular role of HMGB1 in inflammation and sepsis. J. Intern. Med. 255, 320–331.

Wong, D.R., Derijks, L.J., den Dulk, M.O., Gemmeke, E.H., Hooymans, P.M., 2007. The role of xanthine oxidase in thiopurine metabolism: a case report. Ther. Drug Monit. 29, 845–848.

Yano, A., Higuchi, S., Tsuneyama, K., Fukami, T., Nakajima, M., Yokoi, T., 2012. Involvement of immune-related factors in diclofenac-induced acute liver injury in mice. Toxicology 293, 107–114.

Yao, D., Brownlee, M., 2010. Hyperglycemia-induced reactive oxygen species increase expression of the receptor for advanced glycation end products (RAGE) and RAGE ligands. Diabetes 59, 249–255.

Zhao, X., Zhu, J.X., Mo, S.F., Pan, Y., Kong, L.D., 2006. Effects of cassia oil on serum and hepatic uric acid levels in oxonate-induced mice and xanthine dehydrogenase and xanthine oxidase activities in mouse liver. J. Ethnopharmacol. 103, 357–365.

1521-009X/42/1/1–8$25.00
DRUG METABOLISM AND DISPOSITION
http://dx.doi.org/10.1124/dmd.113.054478
Drug Metab Dispos 42:1–8, January 2014

Evaluation and Mechanistic Analysis of the Cytotoxicity of the Acyl Glucuronide of Nonsteroidal Anti-Inflammatory Drugs

Taishi Miyashita, Kento Kimura, Tatsuki Fukami, Miki Nakajima, and Tsuyoshi Yokoi

Drug Metabolism and Toxicology, Faculty of Pharmaceutical Sciences, Kanazawa University, Kanazawa, Japan

Received August 23, 2013; accepted October 8, 2013

ABSTRACT

The chemical reactivity of acyl glucuronide (AG) has been thought to be associated with the toxic properties of drugs containing carboxylic acid moieties, but there has been no direct evidence showing that AG formation is related to the observed toxicity. In the present study, the cytotoxicity of AGs, especially that associated with the inflammatory response, was investigated. The changes in the mRNA and protein expression levels of interleukin 8 (IL-8) and monocyte chemoattractant protein (MCP)-1 induced by the treatment of human peripheral blood mononuclear cells (PBMCs) with diclofenac (Dic), probenecid (Pro), tolmetin (Tol), ibuprofen (Ibu), naproxen (Nap), and their AGs were investigated by real-time reverse transcription polymerase chain reaction, and the viabilities of CD3+, CD14+, and CD19+ cells were measured by flow cytometry. Treatment with Dic-AG, Pro-AG, and Tol-AG significantly increased the expression levels of IL-8 and MCP-1. In addition, Dic-AG, Pro-AG, and Tol-AG significantly decreased the viability of CD14+ cells. Of these three AGs, Dic-AG showed the most potent changes, followed by Tol-AG and Pro-AG. Treatment with Ibu-AG and Nap-AG affected neither the expression levels of IL-8 and MCP-1 nor the viability of CD14+ cells. None of the drugs affected the CD3+ and CD19+ cell populations. Dic-AG increased the phosphorylation of p38 mitogen-activated protein (MAP) kinase and c-Jun N-terminal kinase (JNK)1/2. The pretreatment of peripheral blood mononuclear cells (PBMCs) with SB203580 (p38 inhibitor) significantly suppressed the Dic-AG-induced expression of inflammatory factors and cytotoxicity of CD14+ cells. In conclusion, AGs induce inflammatory responses and cytotoxicity against CD14+ cells via the p38 MAPK pathway. These factors may be useful biomarkers for evaluating the toxicity of AGs.

Introduction

Acyl glucuronidation is one of the major metabolic routes of drugs that contain carboxylic acid moieties. Glucuronidation is one of the most important phase II metabolic pathways for endogenous and exogenous substrates and is generally considered a detoxification pathway. However, it is well known that acyl glucuronides (AGs) are unstable under physiologic conditions and consequently undergo hydrolysis or intramolecular rearrangement through the migration of the drug moiety from the 1-*O*-position to the 2-, 3-, and 4-positions on the glucuronic acid ring (Smith et al., 1990; Benet et al., 1993; Bailey and Dickinson, 2003). AGs covalently modify endogenous proteins due to their electrophilic capacity to cause substitution reactions with the nucleophilic groups located on proteins or other macromolecules, and this effect can ultimately lead to adverse drug toxicities associated with carboxylic acid–containing drugs (Faed, 1984; Boelsterli, 2002). To date, both direct toxic effects and immune-mediated toxicity have been suggested as possible mechanisms of idiosyncratic liver injury. With direct toxicity, covalent protein binding via AG may disrupt the normal physiologic function of a "critical" protein or some critical regulatory pathway that lead to cellular necrosis (Pirmohamed et al., 1996). In addition, it has been reported that electrophilic AGs can covalently interact with nucleic acids. Clofibrate AG and gemfibrozil AG can form DNA adducts that result in genotoxicity, and these adducts can be measured through a single-cell gel electrophoresis (comet) assay (Sallustio et al., 2006). Furthermore, probenecid and clofibric acid have been found to induce DNA damage in isolated hepatocytes and uridine diphosphate (UDP)-glucuronosyltransferase (UGT)-transfected human embryonic kidney (HEK)293 (HEK/UGT) cells via a glucuronidation-dependent pathway (Sallustio et al., 2006; Southwood et al., 2007). Thus, there is increasing evidence that the formation of drug-protein adducts is involved in idiosyncratic reactions. However, we previously reported that the AGs of naproxen, diclofenac, ketoprofen, and ibuprofen do not lead to cytotoxicity or genotoxicity in HEK/UGT cells and human hepatocytes (Koga et al., 2011). Therefore, it is necessary to elucidate the possibility of immune- and/or inflammation-mediated toxicity to clarify the toxicity of AG. The potentially fatal adverse drug reactions most often appear to be immunologically based. These include anaphylactic reactions and severe dermatological reactions, such as Stevens-Johnson syndrome and fatal epidermal necrolysis (Bailey and Dickinson, 2003). In fact, it has been reported that mycophenolic acid, which is the active metabolite of the immunosuppressant mycophenolate mofetil, is primarily metabolized by glucuronidation to form an AG, which was found to result in the induction of cytokine [tumor necrosis

This study was supported by Health and Labor Sciences Research Grants from the Ministry of Health, Labor, and Welfare of Japan (H23-BIO-G001).
dx.doi.org/10.1124/dmd.113.054478.

ABBREVIATIONS: 7AAD, 7-amino-actinomycin D; AG, acyl glucuronide; Dic, diclofenac; ERK, extracellular signal-regulated kinase; GAPDH, glyceraldehyde 3-phosphate dehydrogenase; HEK, human embryonic kidney; Ibu, ibuprofen; IDT, idiosyncratic drug toxicity; IL, interleukin; JNK, c-Jun N-terminal kinase; MAPK, mitogen-activated protein kinase; MCP, monocyte chemoattractant protein; Nap, naproxen; NSAID, nonsteroidal anti-inflammatory drugs; PBMCs, peripheral blood mononuclear cells; PI, propidium iodide; Pro, probenecid; RT-PCR, reverse-transcription polymerase chain reaction; TNF, tumor necrosis factor; Tol, tolmetin; UGT, UDP-glucuronosyltransferase.

factor alpha (TNFα) and interleukin (IL)-6)] formation in leukocytes in a cell-based study (Wieland et al., 2000). It could be envisaged that the induction of immune modulators can lead to immune- and/or inflammation-related adverse drug reactions.

Of the drugs containing carboxylic acid moieties, diclofenac (Dic), probenecid (Pro), tolmetin (Tol), ibuprofen (Ibu), and naproxen (Nap), and their AGs were selected for the present study (Fig. 1). These drugs containing carboxylic acid are associated with some degree of hepatotoxicity, immune cytopenias, and hypersensitivity reactions in patients (Bailey and Dickinson, 2003) and have been categorized as potentially idiosyncratic drug toxicity (IDT) drugs in RxList (the Internet drug index system) or in Japanese drug labeling. Therefore, it is suggested that the AGs of these drugs may be related to their toxicity. The purpose of this study was to investigate whether AGs induce the observed cytotoxicity, particularly through inflammatory responses, and to clarify the involvement of cell signaling in the cytotoxicity.

Materials and Methods

Diclofenac sodium salt (Dic) and (S)-(+)-6-methoxy-α-methyl-2-naphthaleneacetic acid (Nap) were purchased from Sigma-Aldrich (St. Louis, MO). Ibuprofen (Ibu) and probenecid (Pro) were purchased from Wako Pure Chemicals (Osaka, Japan). Tolmetin (Tol) was purchased from LKT Laboratories (St. Paul, MN). 4′-Hydroxy diclofenac (4′-OH Dic), 5-hydroxy diclofenac (5-OH Dic), diclofenac acyl-β-D-glucuronide (Dic-AG), and other AGs were obtained from Toronto Research Chemicals (North York, ON, Canada). Propidium iodide (PI) and 7-amino-actinomycin D (7-AAD) were purchased from BD Pharmingen (San Diego, CA). Monoclonal antibodies against extracellular signal-regulated kinase (ERK)1/2 and c-Jun N-terminal kinase (JNK)1/2 and the polyclonal antibody against p38 mitogen-activated protein kinase (MAPK) were purchased from Cell Signaling Technology (Beverly, MA). Monoclonal antibodies against anti-Thr202/Tyr204 phosphorylated ERK1/2, anti-Thr180/Tyr182 phosphorylated p38 MAPK, and anti-Thr183/Tyr185 phosphorylated JNK1/2 were also obtained from Cell Signaling Technology. IRDye680-labeled goat anti-rabbit or anti-mouse secondary antibody and Odyssey Blocking Buffer were purchased from Li-COR Biosciences (Lincoln, NE). All of the primers were commercially synthesized at Hokkaido System Sciences (Sapporo, Japan). All other reagents were of the highest commercially available grade.

Cell Culture. The human monocytic leukemia cell line THP-1 was obtained from Riken Gene Bank (Tsukuba, Japan). Human peripheral blood mononuclear cells (PBMCs; lot no. 48) and CTL-Test medium for the culture of PBMCs were obtained from Cellular Technology (Shaker Heights, OH). Human "total liver cells" (primary culture of the mixed population of all native human liver cells) were obtained from SciKon Innovation (Chapel Hill, NC). The THP-1 cells were cultured in RPMI 1640 medium (Nissui Pharmaceutical, Tokyo, Japan) supplemented with 10% fetal bovine serum (FBS; Invitrogen, Carlsbad, CA). The total liver cells were cultured in Hepatocyte Basal Medium (HBM) supplemented with Hepatocyte Culture Media (HCM) SingleQuots (Lonza, Basel, Switzerland), and these cells were maintained at 37°C under an atmosphere of 5% CO_2.

The THP-1 cells, PBMCs, and total liver cells were seeded at densities of 1×10^6, 3×10^6, and 7.5×10^5 cells/well, respectively, in a 24-well plate with medium containing the indicated concentration of the selected carboxylic acid–containing drugs and their AG and then incubated at 37°C. The final concentration of methanol in the culture medium was 0.1% in all of the experiments. The supernatants were separated from the cell cultures by centrifugation and stored at –80°C until assayed.

Real-Time Reverse Transcription Polymerase Chain Reaction. The total RNA was extracted from each cell using RNAiso (Takara Bio, Shiga, Japan) according to the protocol supplied by manufacturer. The reverse transcription was performed with ReverTra Ace (Toyobo, Tokyo, Japan) according to the manufacturer's protocol. For quantitative analysis of the mRNA levels of inflammatory cytokines, real-time reverse transcription polymerase chain reaction (RT-PCR) was performed using an MX3000P real-time PCR system (Stratagene, La Jolla, CA). The primers used in this study were human IL-8 (forward: 5′-CAGCCTTCCTG ATTTCTCTGCAG-3′, reverse: 5′-AGACAGAGCTCTCTTCCATCAG-3′) and human monocyte chemoattractant protein (MCP)-1 (forward 5′-ACCGAGAGGCTGAGACTAAC-3′, reverse: 5′-CAGGTGACTGGGGCATTGAT-3′). A 1-μl volume of the reverse-transcribed mixture was added to a PCR mixture containing 10 pmol of each primer and 10 μl of SYBR Premix ExTaq solution; the final volume of the reaction mixture was 20 μl. After an initial denaturation at 95°C for 30 seconds, the amplification was performed through 45 cycles of either denaturation at 94°C for 20 seconds and annealing and extension at 64°C for 20 seconds or denaturation at 94°C for 5 seconds, annealing at 64°C for 10 seconds, and extension at 74°C for 20 seconds. To normalize the RNA loading and PCR variations, the signals of the targets were normalized to the signals of human glyceraldehyde 3-phosphate dehydrogenase (GAPDH) mRNA (forward: 5′-CCATGAGAAGTATGACAACAGCC-3′, reverse: 5′-TGGGTGGCAGTGATGGCATGGA-3′).

Enzyme-Linked Immunosorbent Assay. The levels of the inflammatory chemokines IL-8 and MCP-1 in the cell supernatants were measured using the Human IL-8 ELISA Ready-SET-GO! and Human CCL2 (MCP-1) ELISA Ready-SET-GO! kits (eBioscience, San Diego, CA), respectively, according to the manufacturer's instructions.

Immunoblot Analysis. SDS-polyacrylamide gel electrophoresis and immunoblot analysis were performed. The cell homogenates (30 μg) were separated on 10% polyacrylamide gels and electrotransferred onto polyvinylidene difluoride membranes (Immobilon-P; Millipore Corporation, Billerica, MA). The membranes were probed with the monoclonal antibodies against anti-Thr202/Tyr204–phosphorylated ERK1/2, anti-Thr180/Tyr182–phosphorylated p38 MAPK, and anti-Thr183/Tyr185–phosphorylated JNK1/2 and

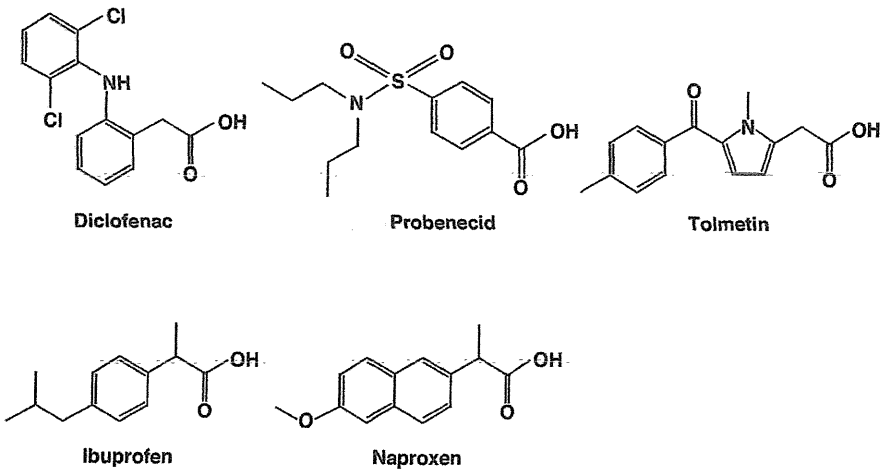

Fig. 1. Chemical structures of the NSAIDs investigated in this study: diclofenac, probenecid, tolmetin, ibuprofen, and naproxen.

incubated with IRDye680-labeled goat anti-rabbit or anti-mouse IgG secondary antibody diluted with phosphate-buffered saline with Tween-20. An Odyssey Infrared Imaging system (Li-COR Biosciences, Lincoln, NE) was used for the detection. The relative expression levels were quantified using the ImageQuant TL Image Analysis software (GE Healthcare, Little Chalfont, Buckinghamshire, UK).

Flow Cytometry Analysis. The PBMCs were washed with phosphate-buffered saline containing 0.1% bovine serum albumin. The cells were transferred to a 96-well plate and maintained on ice throughout the procedure until their analysis by flow cytometry. The PBMCs were stained using the following monoclonal antibodies: anti-human CD3-Pacific Blue (clone UCHT1; Invitrogen, Carlsbad, CA), anti-human CD14-PE (clone TüK4; Invitrogen) anti-human CD19-PE-Cy7 (clone SJ25-C1; Invitrogen). The monoclonal antibodies were diluted 1:10 in phosphate-buffered saline/0.1% bovine serum albumin, and the PBMC were incubated with these antibodies for 30 minutes in the dark. The PBMCs were washed and subsequently incubated with PI (0.625 μg/ml) or 7-AAD (0.25 μg/ml), and the cell viability was measured using an Attune Acoustic Focusing Cytometer (Applied Biosystems, Foster, CA).

Statistical Analyses. The data are presented as the means ± S.D. The comparison of the multiple groups was performed using analysis of variance (ANOVA) followed by the Dunnett or Tukey test. Differences with a P value of less than 0.05 were considered statistically significant.

Results

Effects of Dic-AG on mRNA Expression Levels of IL-8 and MCP-1 in THP-1 Cells, PBMCs, and Total Liver Cells. To investigate whether Dic-AG affects the expression levels of IL-8 and MCP-1 in THP-1 cells, PBMC, and total liver cells, the cells were treated with 100 μM Dic or Dic-AG for 24 hours, and the increase in the IL-8 and MCP-1 mRNA levels was measured. In THP-1 cells and PBMCs, the expression levels of IL-8 and MCP-1 were significantly increased by treatment with Dic-AG but not with vehicle (Ctl) or Dic (Fig. 2, A and B). The changes in the expression levels of these cytokines were higher in PBMCs compared with THP-1 cells: IL-8 (8.3-fold versus 1.7-fold) and MCP-1 (8.5-fold versus 4.7-fold). The total liver cells showed no response to Dic-AG (Fig. 2C). It was suggested that Dic-AG induced immune responses, although the changes in the expression levels of IL-8 and MCP-1 by Dic-AG were different in different cell types. PBMCs were used for the subsequent analyses because these cells demonstrated the highest sensitivity to AGs.

Dose- and Time-Dependent Effects of Dic-AG on IL-8 and MCP-1 mRNA Expression in and Protein Release from Human PBMCs. To investigate whether a low concentration of Dic-AG can affect the expression levels of inflammatory factors in PBMCs, these cells were treated with Dic, Dic-AG (0, 50, or 100 μM), or vehicle (1% methanol, Ctl) for 24 hours. As shown in Fig. 3A, Dic-AG increased the mRNA expression levels of IL-8 and MCP-1 in a dose-dependent manner. The time-dependent changes in the levels of IL-8 and MCP-1 mRNA in PBMCs after treatment with Dic-AG were investigated. Treatment with Dic-AG significantly increased the mRNA expression levels and the release of IL-8 and MCP-1 12 and 24 hours after treatment compared with those observed after treatment with Dic and vehicle (Fig. 3B). The time-dependent changes in the IL-8 and MCP-1 mRNA levels were reflected at the protein level (Fig. 3C); thus, the subsequent experiments mainly analyzed the changes in mRNA expression.

Effects of Dic-AG on Cell Populations of Human PBMCs. The effect of Dic-AG on the major cell populations of PBMCs (monocytes, T-lymphocytes, and B-lymphocytes) was investigated by flow cytometric analysis. The PBMCs were stained with fluorescent monoclonal antibodies against CD3 (T-lymphocyte), CD14 (monocyte), and CD19 (B-lymphocyte) and labeled with 7AAD or PI to detect the dead

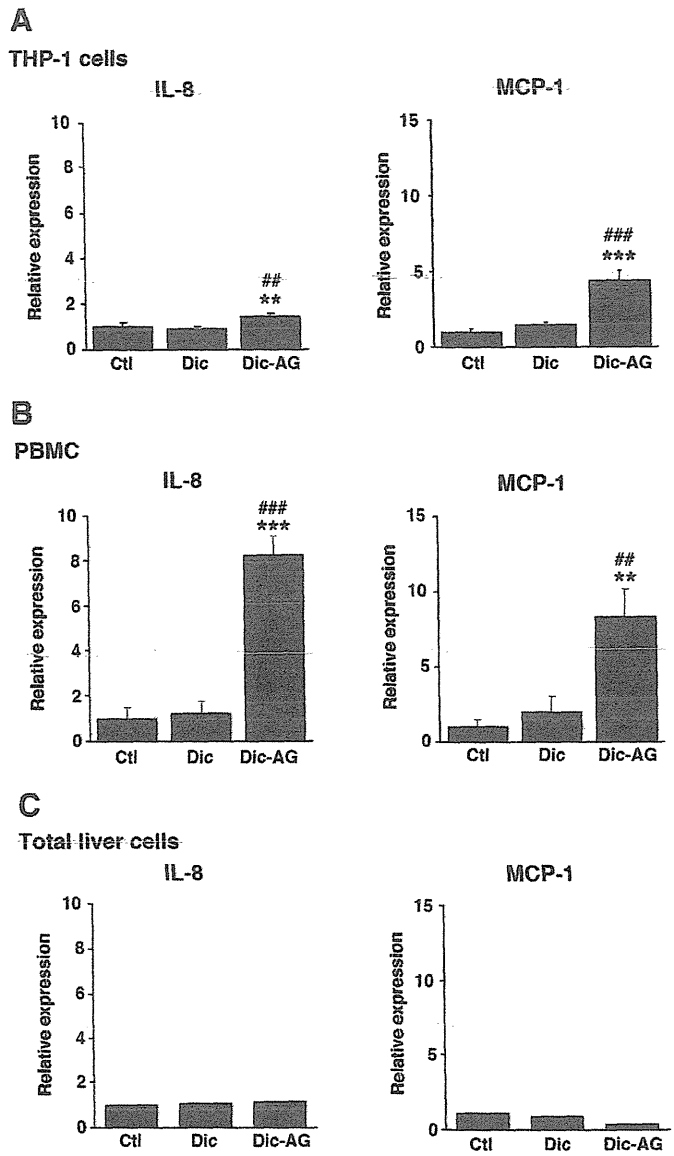

Fig. 2. Effects of Dic-AG on the expression levels of IL-8 and MCP-1 mRNA in THP-1 cells (A), human PBMCs (B), and total liver cells (C). The cells was treated with Dic, Dic-AG (100 μM), or vehicle (1% methanol, Ctl) for 24 hours. The IL-8 and MCP-1 mRNA levels were measured by real-time RT-PCR and normalized with GAPDH. The data represent the means ± S.D. (n = 4) or the mean (n = 2). $^{**}P < 0.01$ and $^{***}P < 0.001$ compared with Ctl. $^{\#\#}P < 0.01$ and $^{\#\#\#}P < 0.001$ compared with Dic.

cells. Treatment with Dic-AG markedly decreased the subset of $CD14^+$ cells of the total cells in a dose- and time-dependent manner (Fig. 4). This effect was not observed with Dic treatment. In addition, Dic-AG showed no inhibitory effect on either the $CD3^+$ cell population or the $CD19^+$ cell population (Fig. 4). These results suggest that Dic-AG specifically affects the viability of $CD14^+$ cells.

Effects of Various AGs on the mRNA Expression of IL-8 and MCP-1 in PBMCs and Their Cytotoxicity on $CD14^+$ Cells. To investigate whether various nonsteroidal anti-inflammatory drug (NSAID) AGs increase the expression levels of IL-8 and MCP-1 and decrease the subset of the $CD14^+$ cell population, PBMCs were treated with 100 μM NSAID or its AG for 24 hours; the mRNA levels of IL-8 and MCP-1 were then measured by real-time RT-PCR, and the cell viabilities of $CD3^+$, $CD14^+$, and $CD19^+$ cells were measured by

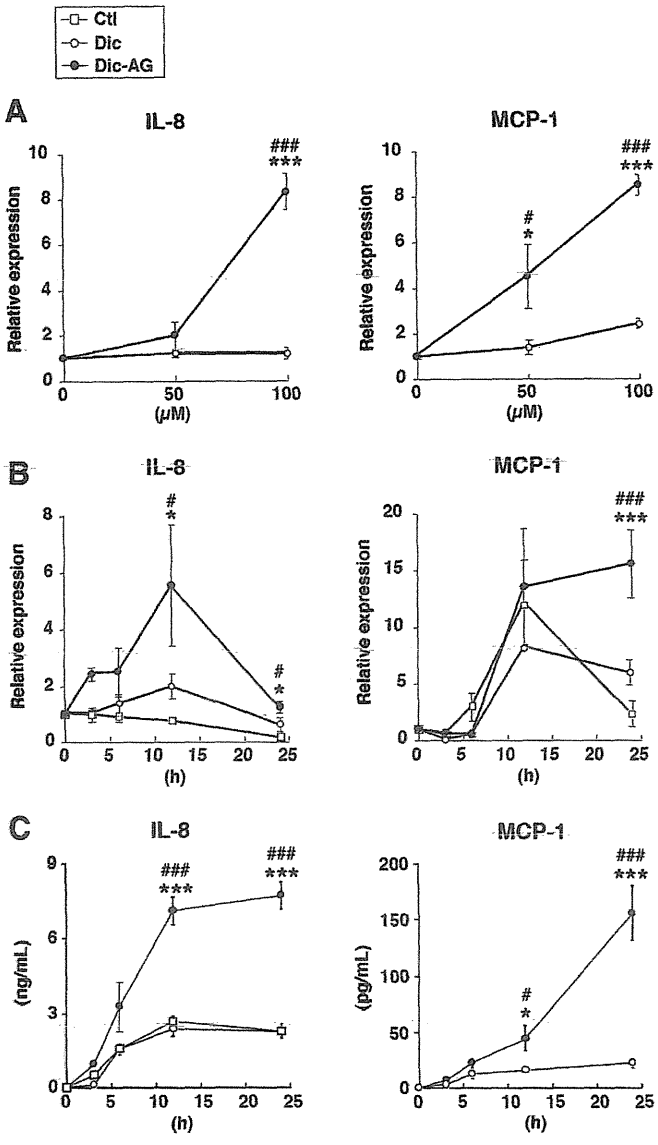

Fig. 3. Dose- and time-dependent effects of Dic-AG on the IL-8 and MCP-1 mRNA expression levels and protein release in human PBMCs. PBMCs were treated with Dic, Dic-AG (0, 50, or 100 μM), or vehicle (1% methanol, Ctl) for 24 hours (A) or with Dic or Dic-AG (100 μM) for 0, 3, 6, 12, and 24 hours (B). The IL-8 and MCP-1 mRNA levels were measured by real-time RT-PCR and normalized with GAPDH. The release of IL-8 and MCP-1 protein into the supernatant was measured by enzyme-linked immunosorbent assay (ELISA) (C). The data represent the means ± S.D. (n = 4). $^{*}P < 0.05$ and $^{***}P < 0.001$ compared with Ctl. $^{\#}P < 0.05$ and $^{\#\#\#}P < 0.001$ compared with Dic.

flow cytometry. As shown in Fig. 5, treatment with Pro-AG, Tol-AG, and Dic-AG significantly increased the expression levels of MCP-1 and IL-8. Furthermore, Pro-AG and Tol-AG significantly decreased the viability of $CD14^+$ cells. Treatment with Ibu-AG and Nap-AG affected neither the expression levels of IL-8 and MCP-1 nor the viability of $CD14^+$ cells. None of the AGs showed an inhibitory effect on either the $CD3^+$ cell population of the $CD19^+$ cell population. These results suggest that the AGs induced inflammatory factors and cytotoxicity against $CD14^+$ cells. Because Dic-AG had a pronounced effect on the expression of inflammatory factors and the viability of $CD14^+$ cells, further studies were performed to analyze the effect of Dic-AG.

Effects of Dic and Its Metabolites on mRNA Expression of IL-8 and MCP-1 and Cell Populations in Human PBMCs. Dic is metabolized to Dic-AG by UGT2B7 and to 4′-hydroxy Dic (4′-OH Dic) and 5-hydroxy Dic (5-OH Dic) by CYP2C9 and CYP3A4, respectively, in humans. It has been reported that these hydroxides are potential protoxicants because they can be further oxidized to quinone imine (van Leeuwen et al., 2011). To investigate whether Dic-AG and other metabolites might increase the expression levels of IL-8 and MCP-1 and decrease the $CD14^+$ cell population in PBMCs, PBMCs were treated with 100 μM Dic-AG, 4′-OH Dic, or 5-OH Dic for 24 hours, and the IL-8 and MCP-1 mRNA levels and the cell viability of $CD3^+$, $CD14^+$, and $CD19^+$ cells were then measured. As shown in Fig. 6, treatment with 4′-OH Dic and Dic-AG significantly increased the expression levels of IL-8 and MCP-1. Furthermore, Dic-AG and 4′-OH Dic significantly decreased the viability of $CD14^+$ cells. None of the compounds decreased the viability of $CD3^+$ and $CD19^+$ cells (data not shown). These results suggest that Dic-AG exhibits the highest cytotoxicity among these metabolites.

Effects of Dic-AG on the Activation of MAPK Signaling Pathways in Human PBMCs. The phosphorylation of MAPKs is a major component of many intracellular signaling pathways. To clarify the MAP kinase activation, the phosphorylation of ERK1/2 (44/42 kDa), p38 MAP kinase (43 kDa), and JNK1/2 (46/54 kDa) in cell lysates was assessed by immunoblot analysis. As shown in Fig. 7, Dic-AG treatment of 0.5 hours significantly increased the phosphorylation of p38 MAP kinase and JNK1/2 but not ERK1/2 in human PBMCs, which suggests that Dic-AG activates the p38 MAP kinase and JNK1/2 pathways in PBMCs. The phosphorylation of ERK1/2 was increased 12 hours after Dic-AG treatment (data not shown). To confirm the effects of MAP kinase inhibitors on the phosphorylation of ERK1/2, p38 MAP kinase, and JNK1/2, PBMC were pretreated for 1 hour with various concentrations of the MAPK/ERK kinase 1/2 inhibitor U0126, the p38 MAP kinase inhibitor SB203580, or the JNK1/2 inhibitor SP600125 before treatment with Dic-AG. The results show that the phosphorylations of p38 MAP kinase and JNK1/2 were significantly suppressed by pretreatment with their specific inhibitors (Fig. 5).

Effects of MAPK Inhibitors on Dic-AG-Induced Inflammatory Factors and Viability of $CD14^+$ Cells in Human PBMCs. To clarify which MAP kinase signaling pathway is mainly involved in the increase in expression levels of IL-8 and MCP-1 and in the decrease of $CD14^+$ cell population in PBMCs, the effects of MAP kinase inhibitors on the expression levels of IL-8 and MCP-1 and the viability of $CD14^+$ cells in PBMCs treated with Dic-AG were investigated. As shown in Fig. 8, the Dic-AG-induced increase in the level of IL-8 mRNA in PBMCs was significantly suppressed by pretreatment with SB203580 and SP600125, and the expression of MCP-1 was significantly suppressed by pretreatment with SB203580 and U0126. These findings suggest that the MAP kinase pathway plays an important role in the expression of IL-8 and MCP-1 in response to Dic-AG treatment. The decreased cell viability of $CD14^+$ cells by Dic-AG treatment was significantly restored by pretreatment with SB203580, which suggests that the p38 MAP kinase pathways are involved in the cytotoxicity of this drug in $CD14^+$ cells (Fig. 8B). These results indicate that the increase in the expression of inflammatory factors by Dic-AG treatment is partly related to the cytotoxic effects observed in $CD14^+$ cells.

Discussion

There is increasing evidence that the formation of drug-protein adducts is involved in idiosyncratic drug toxicities. However, little

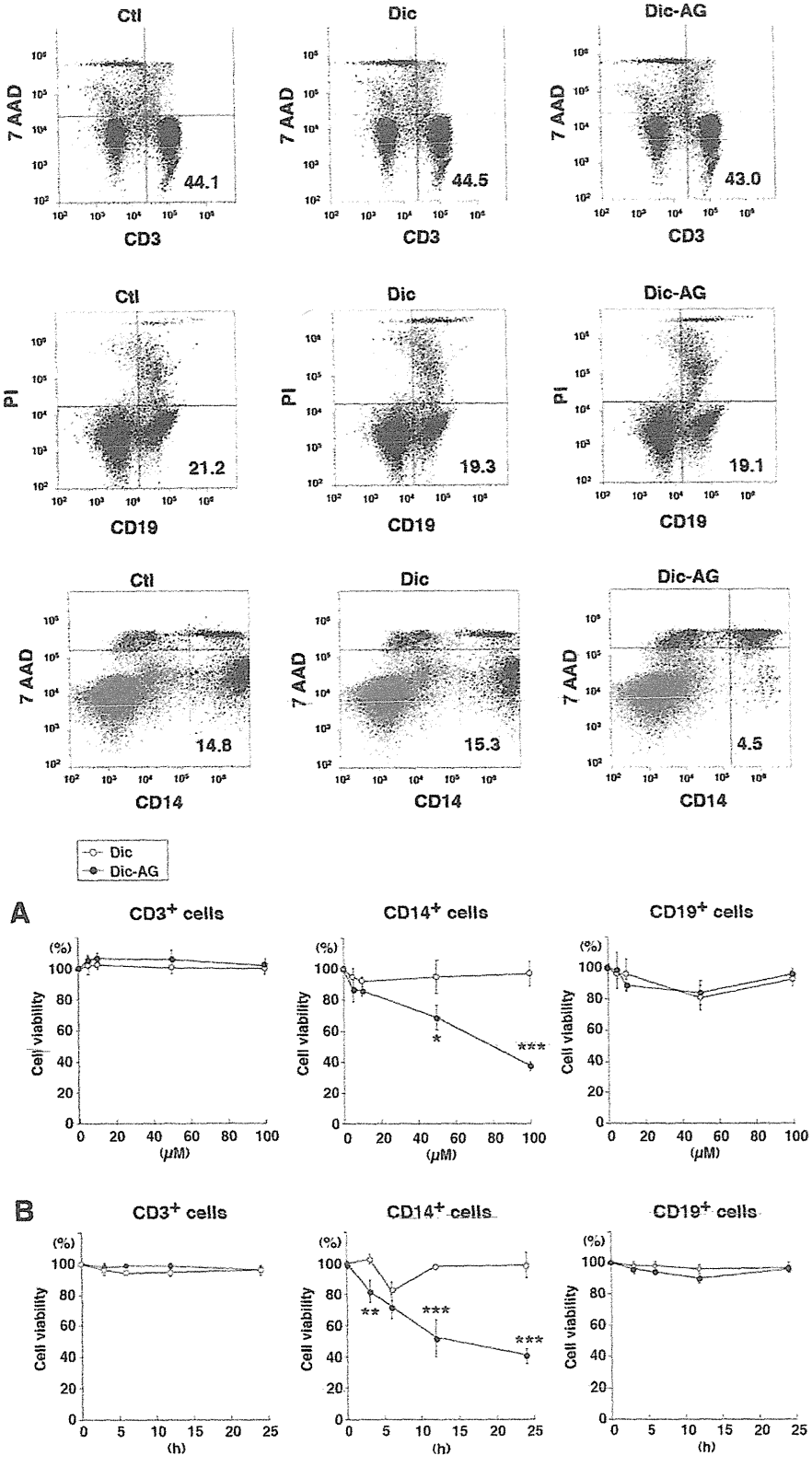

Fig. 4. Flow cytometry analysis of human PBMCs treated with Dic or Dic-AG. Flow cytometric bivariate frequency dot plots showing cell viability of CD3+, CD14, and CD19+ cells in PBMC treated with Dic, Dic-AG (100μM), or vehicle (1% methanol, Ctl) for 24 hours. Human PBMCs were treated with Dic, Dic-AG (0, 50, or 100 μM), or vehicle (1% methanol, Ctl) for 24 hours (A) or with Dic or Dic-AG (100 μM) for 0, 3, 6, 12, and 24 hours (B). The viability of $CD3^+$, $CD14^+$, and $CD19^+$ cells in PBMCs treated with Dic or Dic-AG was measured by PI or 7AAD assay, as described in *Materials and Methods*. The data represent the means ± S.D. ($n = 3$). $^*P < 0.05$, $^{**}P < 0.01$, and $^{***}P < 0.001$ compared with Dic.

direct evidence demonstrates a link between drug-protein adduct formation and adverse biologic consequences. It is well known that AGs are characterized by their electrophilic reactivity, and this reactivity is implicated in a wide range of adverse drug effects, including drug hypersensitivity reactions and cellular toxicity (Ritter, 2000). We previously revealed that the AGs of various NSAIDs, such as naproxen, diclofenac, ketoprofen, and ibuprofen, showed no direct cytotoxicity and genotoxicity in human hepatocytes and cells stably expressing human UGTs (Koga et al., 2011). Therefore, in this study, we investigated whether the AGs exert toxicity through inflammation-

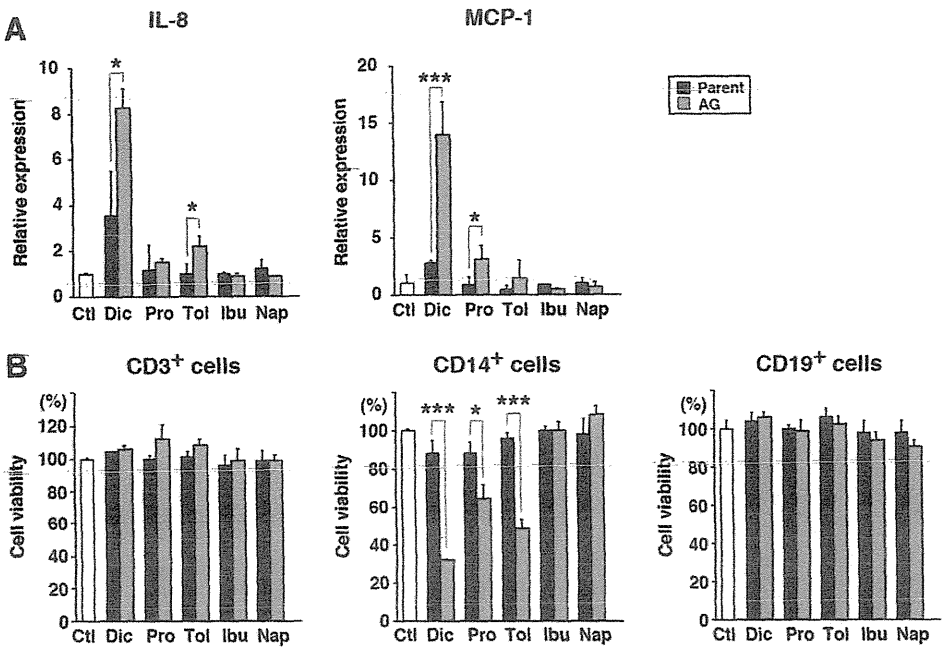

Fig. 5. Effects of NAIDs and their AGs on the mRNA expression levels of IL-8 and MCP-1 and their cytotoxicity to $CD3^+$, $CD14^+$, and $CD19^+$ cells in human PBMCs. Human PBMC were treated with Dic, Dic-AG, Pro, Pro-AG, Tol, Tol-AG, Ibu, Ibu-AG, Nap, Nap-AG (100 μM), or vehicle (1% methanol, Ctl) for 24 hours. The IL-8 and MCP-1 mRNA levels were measured by real-time RT-PCR and normalized with GAPDH (A). The cell viability of $CD14^+$ cells treated with Dic-AG was measured by 7AAD assay as described in *Materials and Methods* (B). The data represent the means ± S.D. (n = 4). $^*P < 0.05$ and $^{***}P < 0.001$ compared with the parent drugs.

related responses. Our previous research revealed that some drugs, such as albendazole, terbinafine, and amiodarone, stimulate THP-1 cells to release IL-8, which suggests the involvement of an inflammation-mediated pathway in drug-induced adverse reactions (Mizuno et al., 2010, 2011; Endo et al., 2012). Furthermore, it has been reported that cytokines and chemokines, such as MCP-1, are released by THP-1 cells and PBMCs after treatment with flavonoids or amyloid proteins (Song et al., 2009). Thus, the expression levels of IL-8 and MCP-1 as markers for predicting the activation of the inflammatory response induced by AGs were investigated in the present study.

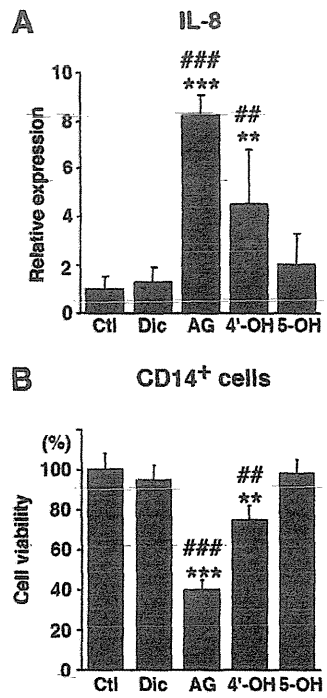

Fig. 6. Effects of Dic and its metabolites on the mRNA expression levels of IL-8 and MCP-1 in human PBMCs. Human PBMCs were treated with Dic, Dic-AG, 4′-OH Dic, 5-OH Dic (100 μM), or vehicle (1% methanol, Ctl) for 24 hours. The expression levels of IL-8 and MCP-1 mRNA were measured by real-time RT-PCR and normalized with GAPDH. The data represent the means ± S.D. (n = 4). $^{**}P < 0.01$ and $^{***}P < 0.001$ compared with Ctl. $^{\#\#}P < 0.01$ and $^{\#\#\#}P < 0.001$ compared with Dic.

First, the effects of Dic-AG treatment on three different types of cells, namely THP-1 cells, PBMCs, and total liver cells, were compared. We previously revealed that the NSAID AGs that were produced in the cells are efficiently released from the cells into the culture medium (Koga et al., 2011). Thus, the effect of AGs was evaluated by exposing the AGs to the outside of the cells, i.e., the culture medium. In a preliminary study, we found that Dic-AG treatment increases IL-8 production in human PBMCs (data not shown). Therefore, three cell types, namely THP-1 cells, PBMCs, and total liver cells, were exposed to Dic-AG treatment, and the treatment effects were compared. The expression levels of IL-8 and MCP-1 were significantly increased in THP-1 cells and PBMCs but not in total liver cells (Fig. 2). It has been reported that some inflammatory factors, such as IL-8, IL-10, and MCP-1, are released from mixed cell culture at a much higher level than that obtained from pure monocytes treated with proteins or chemicals (Feng et al., 2008). In addition, it has been reported that primary PBMCs are more sensitive to drugs and/or chemicals than tumor cells (Hougee et al., 2005). In this study, as suggested by previous reports, the inducibility of IL-8 and MCP-1 in PBMCs by Dic-AG treatment was much higher than that observed in THP-1 cells. We intended to evaluate the inflammatory responses in the liver by using total liver cells. However, the total liver cells are less sensitive to Dic-AG compared with THP-1 cells and PBMCs. The total liver cells were a primary culture of the mixed population of all native human liver cells, consisting mainly of hepatocytes and containing a low percentage of immune-related cells. From the present result, it was suggested that the total liver cells were not suitable for the sensitive in vitro cell-based assay.

Of the commercially available NSAID AGs, Dic-AG, Pro-AG, and Tol-AG induced the expression of IL-8 and MCP-1 and decreased the viability of $CD14^+$ cells. However, Ibu-AG and Nap-AG had no effect (Figs. 4 and 5). It was reported that the half-lives of Dic-AG, Pro-AG, and Tol-AG in potassium phosphate solution or human serum albumin

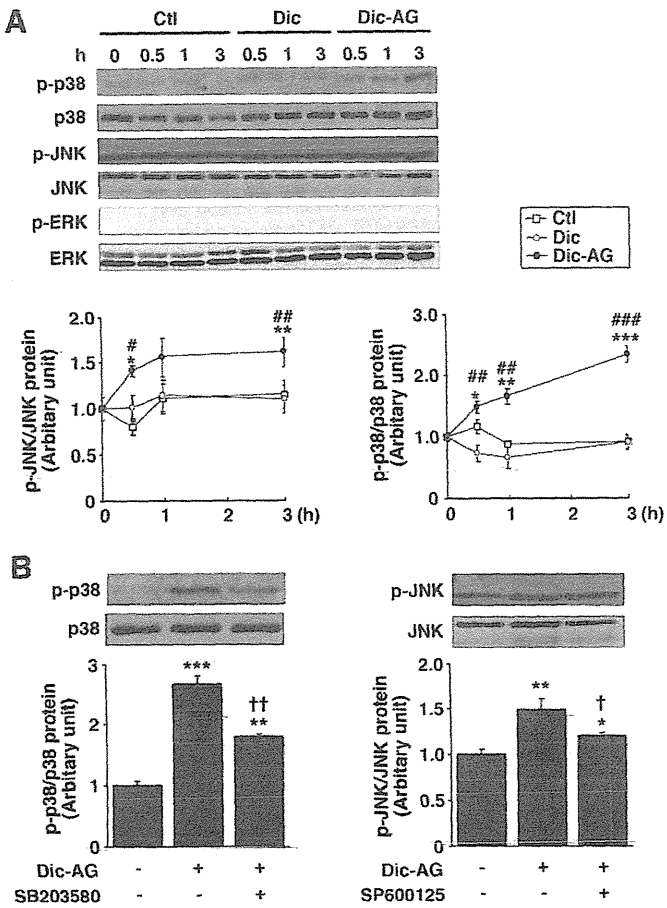

Fig. 7. Activation of MAP kinase signaling pathways in PBMCs treated with Dic-AG. Immunoblot analyses of the MAP kinase proteins in PBMCs were performed and quantified (A). Before treatment with 100 μM Dic-AG, the PBMCs were pretreated with the indicated concentrations of the MAP kinase inhibitors for 1 hour (B). U0126, SB203580, and SP600125 were used as specific inhibitors of MAPK/ERK kinase 1/2, p38 MAP kinase, and JNK1/2, respectively. After 0.5, 1, and 3 hours of incubation with Dic-AG, the cell lysates were subjected to immunoblot analyses using anti-Thr202/Tyr204 phosphorylated ERK1/2, anti-Thr180/Tyr182 phosphorylated p38 MAP kinase, and anti-Thr183/Tyr185 phosphorylated JNK1/2 antibodies. The data represent the means ± S.D. ($n = 3$). $^{*}P < 0.05$, $^{**}P < 0.01$, and $^{***}P < 0.001$ compared with Ctl. $^{\#}P < 0.05$, $^{\#\#}P < 0.01$, and $^{\#\#\#}P < 0.001$ compared with Dic. $^{\dagger}P < 0.05$ and $^{\dagger\dagger}P < 0.01$ compared with Dic-AG.

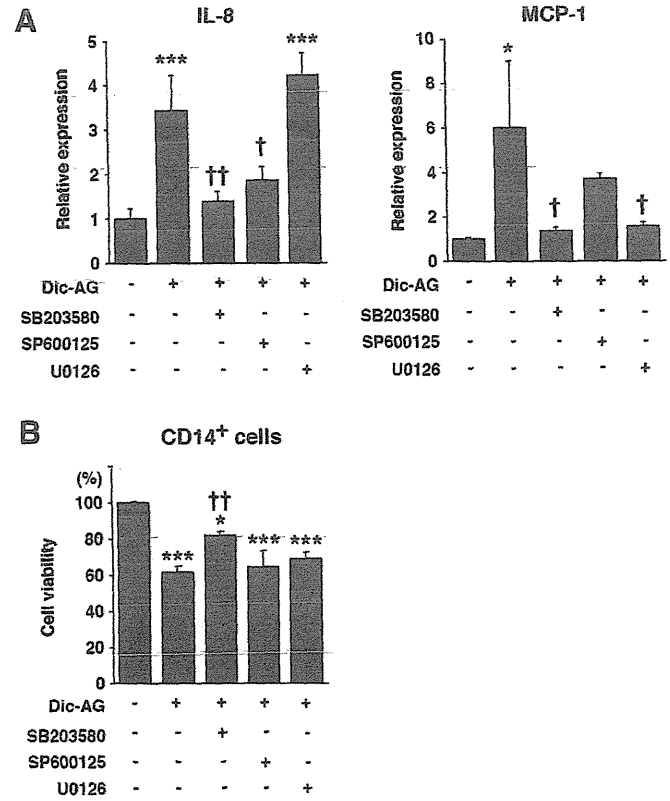

Fig. 8. Effects of MAP kinase inhibitors on Dic-AG-induced IL-8 and MCP-1 expression and cytotoxicity to $CD14^{+}$ cells in human PBMCs. Before treatment with 100 μM Dic-AG, the PBMCs were pretreated with the indicated concentrations of the MAP kinase inhibitors for 1 hour. After 24-hour incubation with Dic-AG, the expression levels of IL-8 and MCP-1 mRNA were measured by real-time RT-PCR, and the viability of $CD14^{+}$ cells treated with Dic-AG was measured by 7AAD assay as described in *Materials and Methods*. The data represent the means ± S.D. ($n = 3$). $^{*}P < 0.05$ and $^{***}P < 0.001$ compared with Ctl. $^{\dagger}P < 0.05$ and $^{\dagger\dagger}P < 0.01$ compared with Dic-AG.

are shorter than those of Ibu-AG and Nap-AG (Sawamura et al., 2010). Furthermore, a covalent binding study using a small peptide demonstrated that the degree of AG reactivity is affected by its chemical structure (Wang et al., 2004) (in descending order): acetic acid derivative > isopropionic acid derivative > benzoic acid derivative. It was hypothesized that the benzoic acid derivative exhibits the lowest reactivity due to the resonance stabilization provided by the aromatic moiety and that the isopropionic acid derivative displays a lower reactivity than that of the acetic acid derivative likely due to the higher steric hindrance capacity of the isopropyl group compared with the acetyl group (Wang et al., 2004). These reports suggest that the stability of AGs serve as a useful key predictor for their IDT risk. Thus, it was surmised that the observed increase in the levels of inflammatory factors and the cytotoxicity of $CD14^{+}$ cells by Dic-AG, Pro-AG, and Tol-AG may be related to the structural properties of the AGs.

Dic-AG is one of the most studied AGs due to its related toxicity. Dic-AG is excreted into bile and transported to the small intestine, where it can produce erosions and ulcers in a dose-dependent manner in rats (Seitz and Boelsterli, 1998). Dic is metabolized to Dic-AG by UGT2B7 and to 4′-hydroxy Dic (4′-OH Dic) and 5-hydroxy Dic (5-OH Dic) by CYP2C9 and CYP3A4, respectively. These hydroxides are further metabolized to form benzoquinone imine, which leads to the production of oxidative stress and covalent binding with endogenous proteins (Tang et al., 1999). Of these metabolites, 4′-OH Dic and Dic-AG increased the expression levels of IL-8 and MCP-1 (Fig. 6). The inducibility of these genes by Dic-AG was much higher than that obtained with 4′-OH Dic, which suggests that Dic-AG shows the highest cytotoxicity among these metabolites. It appeared important to evaluate the toxicity of not only the AG but also the quinone imines of Dic.

The activation of MAP kinases, such as ERK1/2, p38 MAP kinase, and JNK1/2, is important for the mediation of the monocyte and macrophage functions, including the activation of various transcription factors, the production of proinflammatory cytokines, and cell death (Payne et al., 1991; Defranco et al., 1998). In this study, Dic-AG activated the p38 MAP kinase and JNK1/2 pathways in PBMCs (Fig. 7A). The blocking of these MAP kinases by several MAP kinase inhibitors prevented the transcription and/or translation of IL-8 and MCP-1 from Lipopolysaccharide-stimulated monocytes and PBMCs (Guha and Mackman, 2001; Islam et al., 2006). To determine the involvement of MAP kinases in the Dic-AG-induced increase in the expression levels of IL-8 and MCP-1 and the cytotoxicity to $CD14^{+}$ cells, blocking studies were performed using specific inhibitors of

these MAP kinases, including U0126, SB203580, and SP600125 (English and Cobb, 2002). In this study, the p38 MAP kinase pathway was shown to be involved in the stimulation of the increase in the expression levels of IL-8 and MCP-1 in PBMCs (Fig. 8A) and the cytotoxicity to $CD14^+$ cells (Fig. 8B). In the future, it should be clarified whether $CD14^+$ monocytes are the main source of cell death–related inflammatory cytokines and chemokines (IL-8 and MCP-1) after treatment of PBMCs with a drug.

Notably, the circulating cell population of monocytes ($CD14^+$ cells) in the blood is continuously supplied in vivo from the bone marrow, and these cells migrate into the tissues (Hougee et al., 2005), which is an effect that cannot be reproduced under in vitro experimental conditions. It is reported that $CD14^+$ cells were specifically eliminated in PBMCs by apigenin and its structural analogs chrysin and luteolin. Thus, it is considered that the structures of the $CD14^+$ cell surface and of the drugs are important for the onset of toxicity. Therefore, the in vivo evaluation of the mechanism through which AGs exert their selective cytotoxicity to $CD14^+$ cells is required.

In conclusion, we demonstrated that AGs increase the inflammatory responses and cytotoxicity of CD14+ cells via the p38 MAP kinase pathway in human PBMCs. These factors could be useful biomarkers for evaluating the toxicity of AGs. This study provides new insights into the evaluation of the toxicity of AGs in drug development.

Authorship Contributions

Participated in research design: Miyashita, Fukami, Nakajima, Yokoi.
Conducted experiments: Miyashita, Kimura.
Contributed new reagents or analytic tools: Miyashita, Yokoi.
Performed data analysis: Miyashita.
Wrote or contributed to the writing of the manuscript: Miyashita, Yokoi.

References

Bailey MJ and Dickinson RG (2003) Acyl glucuronide reactivity in perspective: biological consequences. *Chem Biol Interact* **145**:117–137.

Benet LZ, Spahn-Langguth H, Iwakawa S, Volland C, Mizuma T, Mayer S, Mutschler E, and Lin ET (1993) Predictability of the covalent binding of acidic drugs in man. *Life Sci* **53**: PL141–PL146.

Boelsterli UA (2002) Xenobiotic acyl glucuronides and acyl CoA thioesters as protein-reactive metabolites with the potential to cause idiosyncratic drug reactions. *Curr Drug Metab* **3**: 439–450.

DeFranco AL, Crowley MT, Finn A, Hambleton J, and Weinstein SL (1998) The role of tyrosine kinases and map kinases in LPS-induced signaling. *Prog Clin Biol Res* **397**:119–136.

Endo S, Toyoda Y, Fukami T, Nakajima M, and Yokoi T (2012) Stimulation of human monocytic THP-1 cells by metabolic activation of hepatotoxic drugs. *Drug Metab Pharmacokinet* **27**: 621–630.

English JM and Cobb MH (2002) Pharmacological inhibitors of MAPK pathways. *Trends Pharmacol Sci* **23**:40–45.

Faed EM (1984) Properties of acyl glucuronides: implications for studies of the pharmacokinetics and metabolism of acidic drugs. *Drug Metab Rev* **15**:1213–1249.

Feng Y, Yang X, Liu Z, Liu Y, Su B, Ding Y, Qin L, Yang H, Zheng R, and Hu Z (2008) Continuous treatment with recombinant Mycobacterium tuberculosis CFP-10-ESAT-6 protein activated human monocyte while deactivated LPS-stimulated macrophage. *Biochem Biophys Res Commun* **365**:534–540.

Guha M and Mackman N (2001) LPS induction of gene expression in human monocytes. *Cell Signal* **13**:85–94.

Hougee S, Sanders A, Faber J, Graus YM, van den Berg WB, Garssen J, Smit HF, and Hoijer MA (2005) Decreased pro-inflammatory cytokine production by LPS-stimulated PBMC upon in vitro incubation with the flavonoids apigenin, luteolin or chrysin, due to selective elimination of monocytes/macrophages. *Biochem Pharmacol* **69**:241–248.

Islam Z, Gray JS, and Pestka JJ (2006) p38 Mitogen-activated protein kinase mediates IL-8 induction by the ribotoxin deoxynivalenol in human monocytes. *Toxicol Appl Pharmacol* **213**:235–244.

Koga T, Fujiwara R, Nakajima M, and Yokoi T (2011) Toxicological evaluation of acyl glucuronides of nonsteroidal anti-inflammatory drugs using human embryonic kidney 293 cells stably expressing human UDP-glucuronosyltransferase and human hepatocytes. *Drug Metab Dispos* **39**:54–60.

Mizuno K, Fukami T, Toyoda Y, Nakajima M, and Yokoi T (2010) Terbinafine stimulates the pro-inflammatory responses in human monocytic THP-1 cells through an ERK signaling pathway. *Life Sci* **87**:537–544.

Mizuno K, Toyoda Y, Fukami T, Nakajima M, and Yokoi T (2011) Stimulation of pro-inflammatory responses by mebendazole in human monocytic THP-1 cells through an ERK signaling pathway. *Arch Toxicol* **85**:199–207.

Payne DM, Rossomando AJ, Martino P, Erickson AK, Her JH, Shabanowitz J, Hunt DF, Weber MJ, and Sturgill TW (1991) Identification of the regulatory phosphorylation sites in pp42/mitogen-activated protein kinase (MAP kinase). *EMBO J* **10**:885–892.

Pirmohamed M, Madden S, and Park BK (1996) Idiosyncratic drug reactions. Metabolic bioactivation as a pathogenic mechanism. *Clin Pharmacokinet* **31**:215–230.

Ritter JK (2000) Roles of glucuronidation and UDP-glucuronosyltransferases in xenobiotic bioactivation reactions. *Chem Biol Interact* **129**:171–193.

Sallustio BC, Degraaf YC, Weekley JS, and Burcham PC (2006) Bioactivation of carboxylic acid compounds by UDP-Glucuronosyltransferases to DNA-damaging intermediates: role of glycoxidation and oxidative stress in genotoxicity. *Chem Res Toxicol* **19**:683–691.

Sawamura R, Okudaira N, Watanabe K, Murai T, Kobayashi Y, Tachibana M, Ohnuki T, Masuda K, Honma H, and Kurihara A, et al. (2010) Predictability of idiosyncratic drug toxicity risk for carboxylic acid-containing drugs based on the chemical stability of acyl glucuronide. *Drug Metab Dispos* **38**:1857–1864.

Seitz S and Boelsterli UA (1998) Diclofenac acyl glucuronide, a major biliary metabolite, is directly involved in small intestinal injury in rats. *Gastroenterology* **115**:1476–1482.

Smith PC, Benet LZ, and McDonagh AF (1990) Covalent binding of zomepirac glucuronide to proteins: evidence for a Schiff base mechanism. *Drug Metab Dispos* **18**:639–644.

Song C, Hsu K, Yamen E, Yan W, Fock J, Witting PK, Geczy CL, and Freedman SB (2009) Serum amyloid A induction of cytokines in monocytes/macrophages and lymphocytes. *Atherosclerosis* **207**:374–383.

Southwood HT, DeGraaf YC, Mackenzie PI, Miners JO, Burcham PC, and Sallustio BC (2007) Carboxylic acid drug-induced DNA nicking in HEK293 cells expressing human UDP-glucuronosyltransferases: role of acyl glucuronide metabolites and glycation pathways. *Chem Res Toxicol* **20**:1520–1527.

Tang W, Stearns RA, Bandiera SM, Zhang Y, Raab C, Braun MP, Dean DC, Pang J, Leung KH, and Doss GA, et al. (1999) Studies on cytochrome P-450-mediated bioactivation of diclofenac in rats and in human hepatocytes: identification of glutathione conjugated metabolites. *Drug Metab Dispos* **27**:365–372.

van Leeuwen JS, Vredenburg G, Dragovic S, Tjong TF, Vos JC, and Vermeulen NP (2011) Metabolism related toxicity of diclofenac in yeast as model system. *Toxicol Lett* **200**:162–168.

Wang J, Davis M, Li F, Azam F, Scatina J, and Talaat R (2004) A novel approach for predicting acyl glucuronide reactivity via Schiff base formation: development of rapidly formed peptide adducts for LC/MS/MS measurements. *Chem Res Toxicol* **17**:1206–1216.

Wieland E, Shipkova M, Schellhaas U, Schütz E, Niedmann PD, Armstrong VW, and Oellerich M (2000) Induction of cytokine release by the acyl glucuronide of mycophenolic acid: a link to side effects? *Clin Biochem* **33**:107–113.

Address correspondence to: Tsuyoshi Yokoi, Department of Drug Safety Sciences, Nagoya University Graduate School of Medicine, 65 Tsurumai-cho, Showa-ku, Nagoya,466-8550, Japan. E-mail: tyokoi@med.nagoya-u.ac.jp

TOXICOLOGICAL SCIENCES 136(1), 250–263 2013
doi:10.1093/toxsci/kft184
Advance Access publication August 28, 2013

A Novel Mouse Model for Phenytoin-Induced Liver Injury: Involvement of Immune-Related Factors and P450-Mediated Metabolism

Eita Sasaki,* Kentaro Matsuo,* Azumi Iida,* Koichi Tsuneyama,† Tatsuki Fukami,* Miki Nakajima,* and Tsuyoshi Yokoi*,[1,2]

*Drug Metabolism and Toxicology, Faculty of Pharmaceutical Sciences, Kanazawa University, Kanazawa 920–1192, Japan; and †Department of Diagnostic Pathology, Graduate School of Medicine and Pharmaceutical Science for Research, University of Toyama, Toyama 930-0194, Japan

[1]Present address: Department of Drug Safety Sciences Nagoya University Graduate School of Medicine, Nagoya, 466-8550, Japan
[2]To whom correspondence should be addressed at Department of Drug Safety Sciences Nagoya University Graduate School of Medicine 65 Tsurumai-cho, Showa-ku, Nagoya, 466-8550, Japan. Fax: +81-76-234-4407. E-mail: tyokoi@p.kanazawa-u.ac.jp.

Received May 19, 2013; accepted August 19, 2013

Drug-induced liver injury is an important issue for drug development and clinical drug therapy; however, in most cases, it is difficult to predict or prevent these reactions due to a lack of suitable animal models and the unknown mechanisms of action. Phenytoin (DPH) is an anticonvulsant drug that is widely used for the treatment of epilepsy. Some patients who are administered DPH will suffer symptoms of drug-induced liver injury characterized by hepatic necrosis. DPH-induced liver injury occurs in 1 in 1000 or 1 in 10 000 patients. Clinically, 75% of patients who develop liver injury develop a fever and 63% develop a rash. In this study, we established a mouse model for DPH-induced liver injury and analyzed the mechanisms for hepatotoxicity in the presence of immune-related or inflammation-related factors and metabolic activation. Female C57BL/6 mice were administered DPH for 5 days in combination with L-buthionine-S,R-sulfoximine. Then, the plasma alanine aminotransferase (ALT) levels were increased, hepatic lesions were observed during the histological evaluations, the hepatic glutathione levels were significantly reduced, and the oxidative stress marker levels were significantly increased. The inhibition of cytochrome P450-dependent oxidative metabolism significantly suppressed the elevated plasma ALT levels and depleted hepatic glutathione. Among the innate immune factors, the hepatic mRNA levels of NACHT, LRR, pyrin domain-containing protein 3, interleukin-1β, and damage-associated molecular patterns were significantly increased. Prostaglandin E_1 treatment ameliorated the hepatic injury caused by DPH. In conclusion, cytochrome P450-dependent metabolic activation followed by the stimulation of the innate immune responses is involved in DPH-induced liver injury.

Key Words: **phenytoin; IL-17; hepatotoxicity; glutathione; mouse model.**

Drug-induced liver injury is a serious issue for new drug candidates and for products currently on the market. Phenytoin (5,5-diphenylhydantoin, DPH) is an anticonvulsant drug that is widely used for the treatment of epilepsy. A fraction of patients administered DPH will suffer symptoms of drug hypersensitivity, typically characterized by a rash, lymphadenopathy, fever, and if the drug continues to be used, drug-induced liver injury (Dhar *et al.*, 1974; Haruda, 1979; Taylor *et al.*, 1984). Hepatic necrosis with a prominent inflammatory response occurs 1–8 weeks after exposure in between 1 in 1000 and 1 in 10 000 patients who receive DPH (Mullick and Ishak, 1980). Therefore, DPH-induced liver injury is generally recognized as idiosyncratic.

Generally, reactive metabolite formation followed by covalent binding may be associated with idiosyncratic toxicity via immune mechanisms (Spielberg *et al.*, 1981). The major metabolic pathway of DPH has been well documented. DPH is hydroxylated by cytochrome P450 (CYP) enzymes to form its phenol metabolite, 5-(*p*-hydroxyphenyl-),5-phenylhydantoin (HPPH). HPPH can be further oxidized to form the DPH catechol (Munns *et al.*, 1997). A number of *in vitro* studies show that the DPH catechol can form protein adducts in the liver microsomes of humans and mice and that DPH catechol formation is catalyzed primarily by CYP2C19 and CYP2C9 in humans (Cuttle *et al.*, 2000) and CYP2C11 in rats (Yamazaki *et al.*, 2001). Covalent bond formation is suppressed when low molecular weight thiols such as glutathione (GSH) and cysteine are present in mice microsomes (Roy and Snodgrass, 1990). Considering these *in vitro* reports, we suspect that the CYP-produced reactive metabolite of DPH covalently binding to hepatic proteins may be responsible for DPH-induced idiosyncratic toxicity. However, there are currently no *in vivo* studies on hepatic GSH content or P450 oxidization metabolism in DPH-induced liver injury due to a lack of an appropriate animal model.

Studies have shown that DPH may generate reactive oxygen species (ROS). For example, antioxidants such as superoxide dismutase (SOD), catalase, and GSH confer protection against DPH embryopathy *in vitro* (Winn and Wells, 1995) and *in vivo* (Winn and Wells, 1999). Recently, ROS have been proposed to

play an important role in the activation of the NACHT-, LRR-, and pyrin domain-containing protein 3 (NALP3) inflammasome (Bryant and fitzgerald, 2009; Martinon *et al.*, 2009). The NALP3 inflammasome generates mature interleukin (IL)-1β via proteolytic pathways, and mature IL-1β engages IL-1R-harboring cells and promotes inflammatory responses (Latz, 2010; Schroder and Tschopp, 2010).

The most frequent mechanism of drug-induced liver injury is the CYP-dependent formation of reactive metabolites that cause cell death or immune reactions that amplify tissue trauma. Necrotic cell death triggers a release of damage-associated molecular patterns (DAMPs), such as the S100 protein and high-mobility group box 1 (HMGB1), which activate innate immune cells (Bianchi, 2007; Scaffidi *et al.*, 2002). The activation of innate immune cells by DAMPs occurs through toll-like receptors (TLRs; Schwabe *et al.*, 2006). Cytokines and chemokines, followed by inflammation or the infiltration of lymphocytes to hepatocytes, are involved in immune-mediated hepatotoxicity and are predominantly secreted by immune cells such as T lymphocytes and macrophages (Kita *et al.*, 2001; Oo and Adams, 2010). Cytokine production is induced by the following transcriptional factors: T-box expressed in T cells (T-bet) induces the secretion of interferon-γ and IL-12; GATA-binding domain-3 (GATA-3) induces IL-4, IL-5, and IL-13 production; and retinoid-related orphan receptor (ROR)-γt is indispensable for the differentiation of Th17 cells, which secrete primarily IL-17 (Kidd, 2003; Langrish *et al.*, 2005; Steinman, 2007).

A number of groups including our own have also recently applied a GSH-depleted animal model to both the evaluation of hepatotoxic potential and the analysis of hepatotoxicity in several drugs that produce reactive metabolites, such as acetaminophen (Watanabe *et al.*, 2003), ticlopidine (Shimizu *et al.*, 2011), and methimazole (Kobayashi *et al.*, 2012). In an animal system depleted of GSH by a well-known GSH synthesis inhibitor, L-buthionine-S,R-sulfoximine (BSO), the tissue GSH levels were significantly reduced without any overt toxicity (Watanabe *et al.*, 2003) or any effects on the hepatic microsomal and cytosolic enzymes responsible for drug metabolism (Drew and Miners, 1984; Watanabe *et al.*, 2003).

In this study, we successfully established a DPH-induced liver injury mouse model using wild-type mice treated with DPH and BSO for 5 days. Our data suggest that DPH metabolism by CYPs and the hepatic GSH content are both involved in DPH-induced liver injury. Furthermore, the inflammation and immune factors believed to be involved in DPH-induced liver injury were investigated.

MATERIALS AND METHODS

Chemicals. DPH, BSO, and mephenytoin were purchased from Wako Pure Chemical Industries (Osaka, Japan); 1-aminobenzotriazole (ABT) was purchased from the Tokyo Chemical Industry (Tokyo, Japan). Eritoran was kindly provided by the Eisai Co. (Tokyo, Japan). Prostaglandin E_1 (PGE_1) was purchased from Nippon Chemiphar (Tokyo, Japan). The Fuji DRI-CHEM slides for GPT/ALT-PIII, GOT/AST-PIII, and TBIL-PIII used to measure alanine aminotransferase (ALT), aspartate aminotransferase (AST), and total bilirubin (T-Bil), respectively, were from Fujifilm (Tokyo, Japan). RNAiso was obtained from Nippon Gene (Tokyo, Japan), ReverTraAce was obtained from Toyobo (Tokyo, Japan), and random hexamers and SYBR Premix EX Taq were from Takara (Osaka, Japan). All primers were commercially synthesized at Hokkaido System Sciences (Sapporo, Japan). The monoclonal anti-mouse IL-17 antibody and the monoclonal rat IgG2a isotype used as a control were obtained from R&D Systems (Abingdon, UK). The rabbit polyclonal antibody against myeloperoxidase (MPO) was obtained from DAKO (Carpinteria, CA). The Ready-SET-GO! Mouse IL-17 ELISA Kit and the Mouse IL-1β ELISA Kit were purchased from eBioscience (San Diego, CA). The chicken anti-HMGB1 polyclonal antibody, chicken polyclonal IgY isotype, and HMGB1 ELISA Kit II were obtained from the Sino-Test Corporation (Tokyo, Japan). The other chemicals used were of analytical or the highest commercially available grade.

DPH and BSO treatments. Female C57BL/6JmsSLC mice (8 weeks old, 16–21 g) were obtained from SLC Japan (Hamamatsu, Japan). The mice were housed in a controlled environment at 23°C ± 1°C and 50% ± 10% humidity and with a 12-h light/12-h dark cycle in the institution's animal facility with ad libitum access to food and water. The animals were acclimatized before being used in the experiments. In this study, female C57BL/6J mice were used because female mice showed higher sensitivity to DPH-induced liver injury than male mice (data not shown). Repeated administration of DPH orally at a dose of 100 mg/kg for 6 days caused high mortality (60% of mice were dead on days 1 through 6). We speculated that this high mortality was caused by the pharmacological effects of DPH. DPH is known to induce CYPs (Cyps) in humans (Chaudhry *et al.*, 2010; Fleishaker *et al.*, 1995) and mice (Hagemeyer *et al.*, 2010). Thus, repeated administration of DPH increased DPH metabolism, contributing to the reduction of its pharmacological effects. However, the administration of DPH at a dose of 100 mg/kg for 6 days caused high mortality on days 1 and 2 due to its pharmacological effects. This phenomenon is partially explained by the fact that on days 1 and 2, induction of hepatic Cyps by DPH did not occur or was insufficient. Thus, we thought that the dose amount of DPH on days 1 and 2 should be under 100 mg/kg to reduce mortality. Therefore, we employed a dosing regimen as follows. First, 50 mg/kg of DPH was IP injected for the first 2 days. In this step, we expected to induce the hepatic Cyps by DPH. On days 3 through 5, 100 mg/kg of DPH was orally administered. In this step, we expected that the expression of hepatic Cyps had been induced by 50 mg/kg of DPH during the first 2 days of IP administration. In this dosing regimen, the mortality rate was 10%–20% on days 1 through 5. Thus, the dosage of DPH was increased to 100 mg/kg on days 3 through 5. BSO is generally administered IP. To avoid unexpected adverse interactions between DHP and BSO, we changed the dosing route of DPH on days 3 through 5. Finally, in this study, the mice were IP administered DPH in corn oil at a dose of 50 mg/kg for 2 days followed by oral administration of 100 mg/kg on days 3 through 5. BSO in saline was IP injected at a dose of 700 mg/kg 1 h prior to each DPH administration as reported by Shimizu *et al.* (2011). As a control, mice were injected with corn oil or saline, which were used as the vehicles for DPH and BSO, respectively. To determine the time-dependent changes in the plasma ALT levels, the mice were anesthetized with ether, and then blood was collected at 0 and 6 h after DPH administration on days 1 through 4 and 0, 3, 6, 24, and 48 h after the final DPH administration. Each group included 4–6 mice. At 72 h after the final DPH administration (final time point for blood collection), the blood samples were collected from the inferior vena cava for biochemical analyses. For measurement of the hepatic mRNA expression of immune- and inflammation-related factors, hepatic GSH content, protein carbonyl content, and histopathological analysis, individual mice were investigated at 24 h before (–24) and at 0, 1.5, 3, 6, 12, or 24 h after the final DPH administration. The blood samples were collected from the inferior vena cava for measurement of plasma cytokine levels. A portion of the hepatic left lobe was excised and fixed in 10% neutral buffered formalin for the histopathological examinations. The remaining liver was frozen in liquid nitrogen and stored at −80°C until use for the measurement of mRNA

expression levels, protein carbonyl content, and GSH content. Each treatment group included 3–5 mice in each time point. As a negative control, we chose mephenytoin as a structural homologue of DPH and with similar pharmacological effects to DPH. In addition, mephenytoin-induced liver injury has a low incidence compared with DPH (Zimmerman, 1999). The mice were administered mephenytoin in corn oil using the same dosing regimen as that used for DPH and BSO. To investigate the importance of the repeated administration for developing DPH-induced liver injury, we conducted a single-administration study. To investigate whether liver injury does not occur, the mice were either IP given 50 mg/kg or 100 mg/kg DPH, or they were orally given 100 or 200 mg/kg DPH and euthanized 24 h after drug administration. BSO (700 mg/kg) was IP injected 1 h prior to DPH treatment. A portion of each excised liver was fixed in a 10% formalin neutral buffer solution and used for immunohistochemistry. The degree of liver injury was assessed by hematoxylin and eosin staining and MPO staining. The plasma ALT, AST, and T-Bil levels were measured using DRI-CHEM (Fujifilm). The animals were treated and maintained in accordance with the National Institutes of Health Guide for Animal Welfare of Japan, and the animal protocols were approved by the Institutional Animal Care and Use Committee of Kanazawa University, Japan.

Treatment with ABT. One hour prior to the final DPH treatment, the mice were IP injected with ABT (100 mg/kg in saline) according to the previous studies (Shimizu et al., 2009, 2011). The vehicle was used as a control.

GSH assay. The mouse livers were homogenized in ice-cold 5% sulfosalicylic acid and centrifuged at 8000 × g for 10 min. The supernatant total GSH and glutathione disulfide (GSSG) concentration was measured as previously described (Tietze, 1969). The GSH levels were calculated from the difference between the total GSH and the GSSG concentration.

Protein carbonyl content. Increased protein carbonyls are a stable indicator of oxidative stress. The protein carbonyl content of the liver homogenate was measured using a Protein Carbonyl ELISA kit (Enzo LifeScience, New York). The assay was performed according to the manufacturer's instructions.

Real-time reverse transcription (RT)-PCR. RNA from mouse liver was isolated using RNAiso (Nippon Gene, Tokyo, Japan) according to the manufacturer's instructions. The mRNA levels of S100A8, S100A9, TLR2, TLR4, TLR9, receptor for advanced glycation end products (RAGE), NALP3, IL-1β, IL-23 p19, IL-6, GATA-3, RORγt, forkhead box P3 (Foxp3), Fas, FasL, T-bet, macrophage inflammatory protein-2 (MIP-2), and monocyte chemoattractant protein-1 (MCP-1) were quantified using real-time RT-PCR. For the RT step, total RNA (10 μg) and 150 ng of random hexamers were mixed and incubated at 70°C for 10 min. The RNA solution was added to a reaction mixture containing 100 units of ReverTra Ace, reaction buffer, and 0.5mM deoxyribonucleotide triphosphates at a final volume of 40 μl. The resulting reaction mixture was incubated at 30°C for 10 min, 42°C for 1 h, and heated to 98°C for 10 min to inactivate the enzyme. Real-time RT-PCR was performed using the MX3000P instrument (Stratagene, La Jolla, California). The PCR mixture contained 1 μl of template cDNA, SYBR Premix Ex Taq solution, and 8 pmol each of forward and reverse primers. The amplified products were monitored directly by measuring the increase of the SYBR Green I (Molecular Probes, Eugene, Oregon) dye intensity. The primer sequences are shown in Table 1.

Measurement of plasma HMGB1, IL-17, and IL-1β levels. The plasma levels of HMGB1, IL-17, and IL-1β were measured by ELISA using the HMGB1 ELISA Kit II, a Ready-SET-GO! Mouse IL-17, and a Ready-SET-GO! Mouse IL-1β Kit, respectively, according to the manufacturers' instructions.

Administration of a TLR4 antagonist. The mice were IV treated with eritoran, a TLR4 antagonist (50 μg/mouse in 0.2 ml sterile saline), simultaneously with the final DPH treatment as previously described (Higuchi *et al.*, 2012). The vehicle was used as a control.

Administration of an anti-mouse IL-17 antibody or an anti-mouse HMGB1 antibody. In the IL-17 neutralization study, as described in our previous report (Higuchi *et al.*, 2012), the mice were IV treated with an anti-mouse IL-17 antibody (100 μg anti-mouse IL-17 antibody in 0.2 ml sterile PBS) 3 h after the final DPH treatment. As a control, rat IgG2a was used (100 μg rat IgG2a in 0.2 ml sterile PBS). In the HMGB1 neutralization study, the mice were IV treated with an anti-mouse HMGB1 antibody (200 μg anti-mouse HMGB1 antibody in 0.2 ml sterile PBS) simultaneously with the final DPH treatment. As a control, a chicken IgY isotype was used (200 μg chicken IgY in 0.2 ml sterile PBS).

Quantification of hepatic MPO-positive cells. The infiltration of neutrophils was assessed by immunostaining for MPO. A rabbit polyclonal antibody against MPO was used for the immunohistochemical staining of liver as previously described (Higuchi *et al.*, 2012). Three visual fields of ×400 magnification (0.1 mm^2 each) were randomly selected from each MPO-immunostained section. The total number of MPO-positive mononuclear cells from the 3 randomly selected visual fields was compared among the specimens.

Treatment with PGE1. Three hours after the final DPH treatment, the mice were IP given PGE_1 (at 50 μg/mouse in 0.5 ml sterile saline) as previously described (Higuchi *et al.*, 2012; Kobayashi *et al.*, 2009). The vehicle was used as a control.

Statistical analysis. The data are shown as the mean ± SEM. Statistical analyses of multiple groups were performed using a one-way ANOVA with the Dunnett's post hoc test to determine the significance of the differences between individual groups. Comparisons between 2 groups were carried out using a 2-tailed Student's *t* test. A value of $p < .05$ was considered statistically significant.

RESULTS

Development of a DPH-Induced Liver Injury in C57BL/6 Mice

DPH is widely used as an anticonvulsant drug and rarely causes hepatotoxicity with or without hypersensitivity. To study the mechanism of hepatotoxicity, we developed an animal model for DPH-induced liver injury in mice. The mice were IP given DPH at a dose of 50 mg/kg for 2 days and orally administered 100 mg/kg on days 3 through 5. BSO was given on all days. With this dosing regimen, the ALT levels were significantly increased after the final DPH treatment without a high fatality rate (Fig. 1A, mortality rate was 10%–20% on days 1 through 5). These hepatotoxic effects were observed in approximately 60% of the mice, and the others showed no or mild hepatotoxicity, resulting in large SEM values. Without BSO, the plasma ALT levels were much lower than those in the BSO-treated mice. No significant elevation of ALT levels was observed in mice treated with vehicle or BSO alone (Fig. 1A).

In a single-administration study, the female C57BL/6 mice were orally given DPH at a dose of 100 or 200 mg/kg in combination with BSO. The plasma ALT level was not affected by DPH treatment (Fig. 1B). Next, the mice were IP given DPH at a dose of 50 or 100 mg/kg in combination with BSO, resulting in no hepatotoxicity caused by DPH (Fig. 1B).

Mephenytoin, used as a negative control, did not induce hepatotoxicity under the same dosing regimen as DPH, even when combined with BSO, suggesting that the hepatotoxicity of DPH is independent of its pharmacological effects (Fig. 1C).

In the histopathological experiments, apoptosis and hepatocyte ballooning were observed at 24 h after the final DPH and BSO treatment (Fig. 1D). In addition, immunohistochemistry with an anti-MPO antibody demonstrated that a number of MPO-positive cells had infiltrated in DPH- and BSO-treated mice (Fig. 1D). The

TABLE 1.
Sequences of the Primers Used for Real-time RT-PCR Analyses

Genes		Sequences
FasL	FP	AGA AGG AAC TGG CAG AAC TC
	RP	GCG GTT CCA TAT GTG TCT TC
Foxp3	FP	CTA GCA GTC CAC TTC ACC AAG
	RP	GCT GCT GAG ATG TGA CTG TC
Gapdh	FP	AAA TGG GGT GAG GCC GGT
	RP	ATT GCT GAC AAT CTT GAG TGA
GATA-3	FP	GGA GGA CTT CCC CAA GAG CA
	RP	CAT GCT GGA AGG GTG GTG A
IL-1β	FP	GTT GAC GGA CCC CAA AAG AT
	RP	CAC ACA CCA GCA GGT TAT CA
IL-6	FP	CCA TAG CTA CCT GGA GTA CA
	RP	GGA AAT TGG GGT AGG AAG GA
IL-23 p19	FP	CCA GTG TGA AGA TGG TTG TG
	RP	CTA GTA GGG AGG TGT GAA GT
MIP-2	FP	AAG TTT GCC TTG ACC CTG AAG
	RP	ATC AGG TAC GAT CCA GGC TTC
MCP-1	FP	TGT CAT GCT TCT GGG CTT G
	RP	CCT CTC TCT TGA GCT TGG TG
NALP3	FP	GTT GAC GGA CCC CAA AAG AT
	RP	CAC ACA CCA GCA GGT TAT CA
RAGE	FP	GTG CTG GTT CTT GCT CTA TG
	RP	ATC GAC AAT TCC AGT GGC TG
ROR-γt	FP	ACC TCC ACT GCC AGC TGT GTG CTG TC
	RP	TCA TTT CTG CAC TTC TGC ATG TAG ACT GTC CC
S100A8	FP	GAG TGT CCT CAG TTT GTG CAG
	RP	TAG ACA TAT CCA GGG ACCCAG
S100A9	FP	GAT GGC CAA CAA AGC ACC TT
	RP	CCT CAA AGC TCA GCT GAT TG
T-bet	FP	TGC CCG AAC TAC AGT CAG GAA C
	RP	AGT GAC CTC GCC TGG TGA AAT G
TLR2	FP	GAA AAG ATG TCG TTC AAG GAG
	RP	TTG CTG AAG AGG ACT GTT ATG
TLR4	FP	TTC TTC TCC TGC CTG ACA CC
	RP	CCA TGC CAT GCC TTG TCT TC
TLR9	FP	ATT CTC TGC CGC CCA GTT TGT C
	RP	ACG GTT GGA GAT CAA GGA GAG G

Abbreviations: Foxp3, forkhead box P3; FP: forward primer; GATA-3, GATA-binding domain-3; IL, interleukin; MCP-1, monocyte chemoattractant protein-1; MIP-2, macrophage inflammatory protein-2; NALP3, NACHT-, LRR-, and pyrin domain-containing protein 3; RAGE, receptor for advanced glycation end products; ROR, retinoid-related orphan receptor; RP, reverse primer; T-bet, T-box expressed in T cells; TLR, toll-like receptor.

number of MPO-positive cells was significantly increased in mice given DPH or DPH plus BSO compared with vehicle-treated mice (Fig. 1E). However, liver section of DPH-alone-treated (without BSO) mice were often observed to have mild fat droplets but no apoptotic or ballooning cells, suggesting that the hepatic lesion mainly occurred in mice given both DPH and BSO. No histopathological difference was observed between the vehicle- and BSO-treated mice. Taken together, these results indicate that a DPH-induced liver injury mouse model was established.

Changes in Hepatic GSH and Oxidative Stress Marker Levels

The depletion of hepatic GSH by BSO was expected to exacerbate DPH-induced hepatotoxicity. Therefore, we investigated whether GSH is involved in the detoxification of DPH-induced liver injury. GSH levels were significantly decreased at all time points in mice given both DPH and BSO (Fig. 2A). In mice given only DPH, the GSH levels were significantly lower at 1.5, 3, 6, and 24 h after the final DPH treatment. These results suggest that DPH has the ability to deplete hepatic GSH, leading to the development of DPH-induced hepatotoxicity.

We measured hepatic GSSG, a biomarker of oxidative stress. Changes in hepatic GSSG levels showed a similar profile to that of GSH (Fig. 2A). The total glutathione (GSH+GSSG) levels were significantly lowered in mice treated with DPH alone and DPH and BSO together. The GSH/GSSG ratio, a biomarker of oxidative stress, was significantly lowered 1.5 h after the final DPH treatment in mice given both DPH and BSO. The hepatic protein carbonyl levels, a marker of oxidative stress, were significantly increased 6 h after the final DPH treatment in mice given both DPH and BSO but not in mice given only DPH or vehicle (Fig. 2B). These results suggest that oxidative stress is involved in DPH-induced liver injury and that GSH may have a protective role in DPH-induced liver injury.

Effect of the P450 Inhibitor

To investigate whether P450-mediated metabolism is involved in DPH-induced liver injury, mice were IP given ABT (100 mg/kg), a nonspecific inhibitor of P450, 1 h prior to the final DPH administration. In the ABT-treated mice, the elevated plasma ALT and AST levels were significantly suppressed (Fig. 3A). Treatment with ABT alone or ABT and BSO together (data not shown) did not result in any changes in the ALT or AST levels compared with the vehicle-treated mice.

To confirm the involvement of reactive intermediates in the DPH-induced liver injury, we measured the effects of ABT on the hepatic GSH and GSSG levels. The hepatic GSH depletion caused by DPH was significantly restored by ABT 24 h after the final DPH treatment (Fig. 3B). ABT alone did not change the GSH levels, suggesting that ABT itself does not affect the hepatic GSH levels at this dosing regimen. The hepatic total glutathione (GSH + GSSG) levels had a similar profile to that of GSH, suggesting that GSH may be consumed by P450-mediated reactive metabolites (Fig. 3B). These results suggest that P450-mediated metabolism is involved in DPH-induced liver injury.

Changes in the Expression Levels of DAMP-Related Factors

To investigate whether DAMPs and their receptors are involved in the onset of liver injury, time-dependent changes in the hepatic mRNA expression levels of TLR9, TLR4, TLR2, S100A9, S100A8, and RAGE were measured (Fig. 4A). The mRNA expression level of TLR2 was extremely variable in the treated mice, but it was significantly increased at some time points in response to either DPH or DPH plus BSO. The expression level of S100A8 mRNA was significantly increased

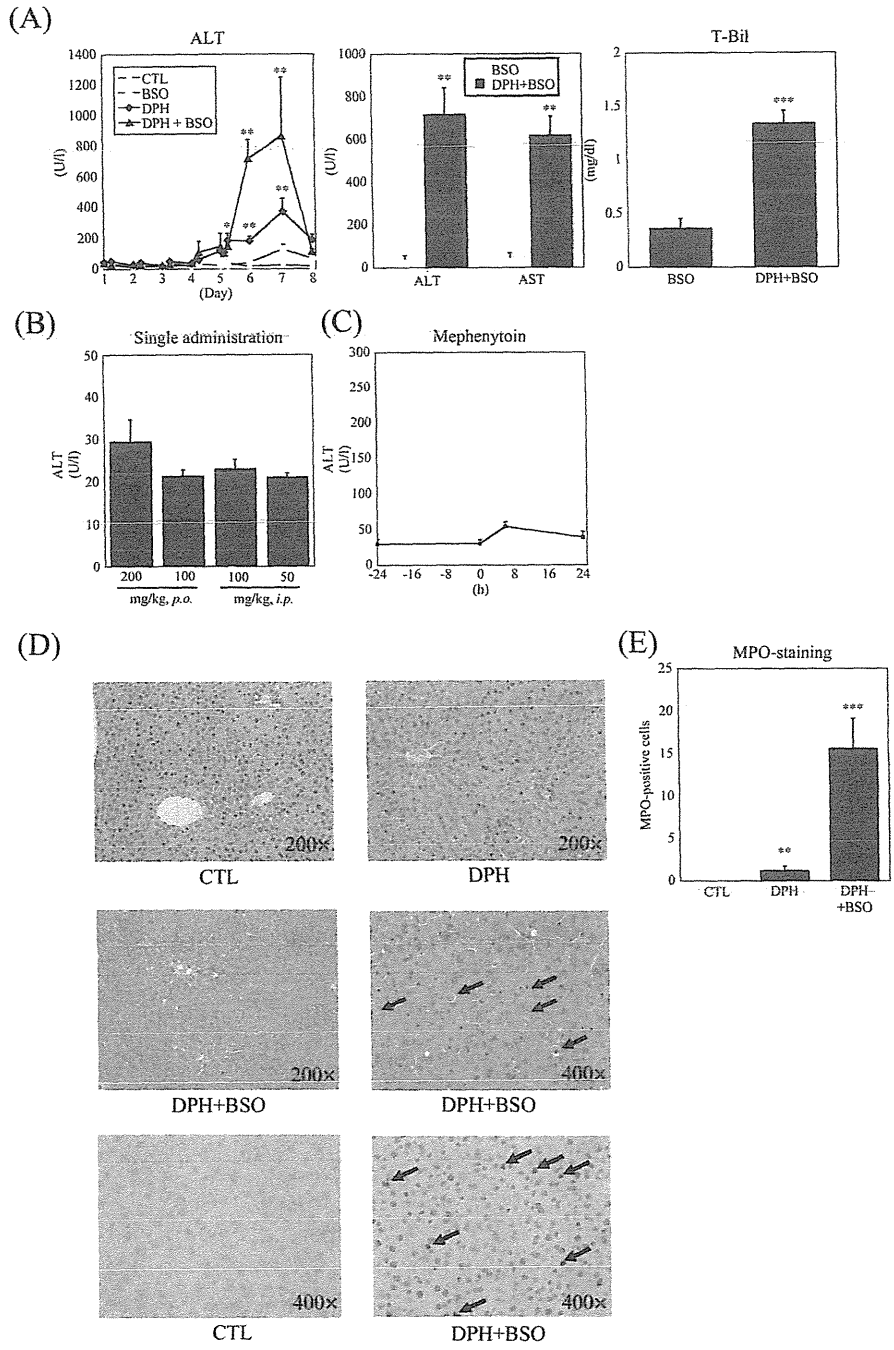

FIG. 1. Time-dependent changes in plasma ALT and AST levels in DPH-induced liver injury. A, Female C57BL/6 mice were IP given DPH at 50 mg/kg for 2 days followed by oral administration of 100 mg/kg DPH on days 3 through 5. BSO (700 mg/kg) was IP injected 1 h prior to each DPH administration. Each vehicle was used as a control. At 0 and 6 h after DPH administration on days 1–4 and at 0, 3, 6, 24, 48, and 72 h after the final DPH treatment, blood was collected to measure the plasma ALT levels. The days 6, 7, and 8 correspond to 24, 48, and 72 h after the final DPH treatment. In the second panel, the plasma ALT, AST, and T-Bil levels were measured 24 h after the final DPH treatment. The values represent the mean ± SEM of 4–6 animals. B, In a single-administration experiment, the mice were given an oral dose of DPH at 200 or 100 mg/kg and an IP injection of 100 or 50 mg/kg. BSO (700 mg/kg) was IP injected 1 h prior to the DPH treatment, and blood was collected 24 h after DPH administration. The values represent the mean ± SEM of 4 animals. C, As the negative control, the mice were given mephenytoin and BSO with the same dosing regimen as in (A). At 24 h before (−24) and 0, 6, and 24 h after the final mephenytoin treatment, blood was collected to measure the plasma ALT levels. Values represent the mean ± SEM of 4 animals. D, Liver tissue sections from 24 h after the final DPH treatment were stained with hematoxylin and eosin. Neutrophil infiltration was assessed by immunostaining for MPO. The arrows indicate apoptosis or MPO-positive cells. E, The number of MPO-positive cells in mice treated with DPH and BSO, DPH alone, or vehicle. Values represent the mean ± SEM of 4–5 specimens. The differences relative to the control mice (MPO-stained) or BSO-treated mice (ALT, AST, and T-Bil) were considered significant at $*p < .05$, $**p < .01$, and $***p < .001$. Abbreviations: ALT, alanine aminotransferase; AST, aspartate aminotransferase; BSO, L-buthionine-S,R-sulfoximine; DPH, 5,5-diphenylhydantoin; T-Bil, total bilirubin.

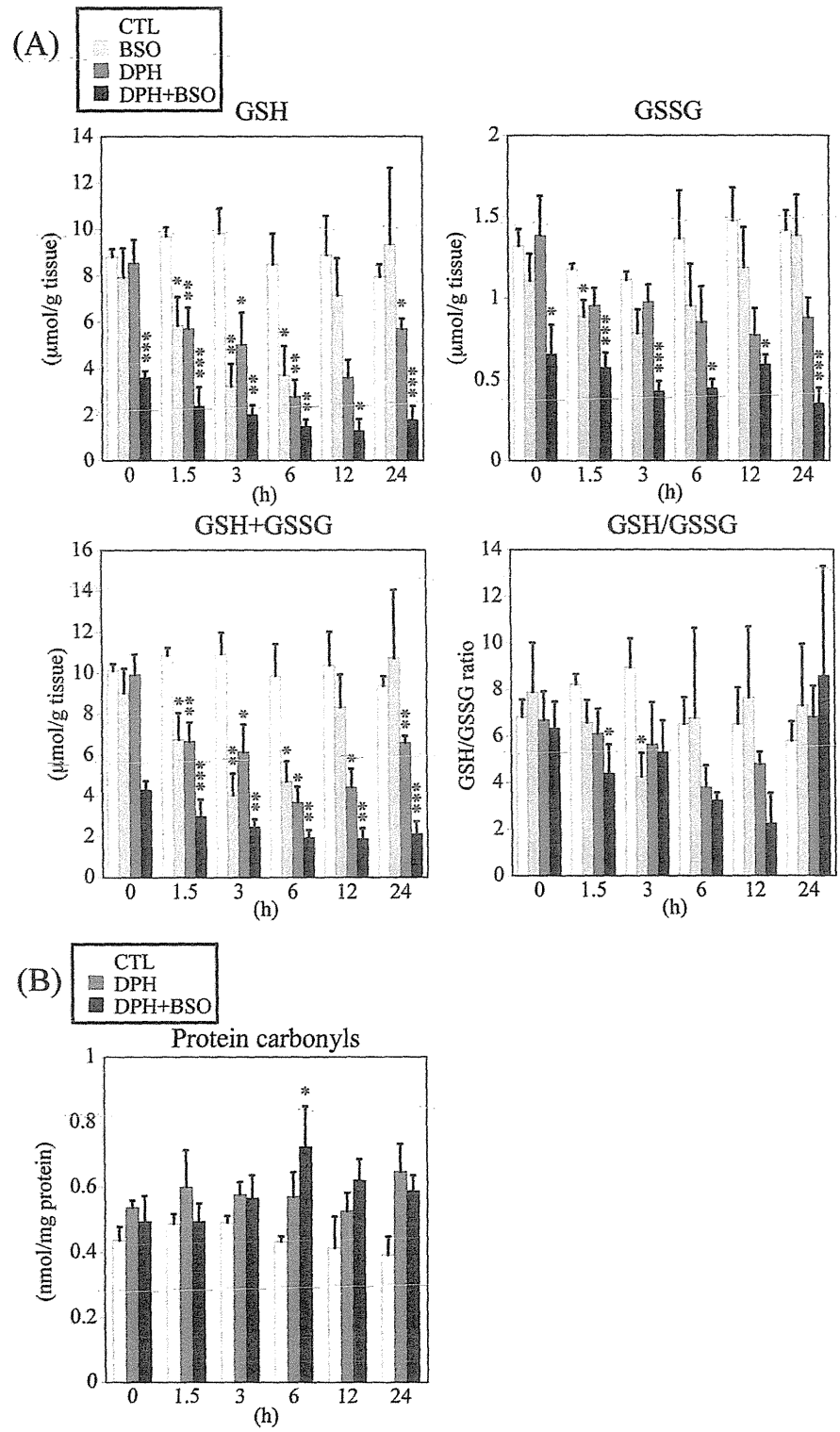

FIG. 2. Time-dependent changes in hepatic GSH, GSSG, and oxidative stress marker in DPH-induced liver injury. The mice were IP given DPH at 50 mg/kg for 2 days, and afterwards on days 3 through 5, DPH was orally administered at 100 mg/kg. BSO was IP injected 1 h prior to each DPH administration. Each vehicle was used as a control. At 0, 1.5, 3, 6, 12, and 24 h after the final DPH treatment, the liver was collected to measure the hepatic GSH, GSSG, and GSH + GSSG levels, the GSH/GSSG ratio (A), and the level of hepatic protein carbonyls (B). The data are shown as the mean ± SEM of the results from 4 to 5 mice. The differences relative to the control mice were considered significant at $*p < .05$, $**p < .01$, and $*** p < .001$. Abbreviations: DPH, 5,5-diphenylhydantoin; GSH, glutathione; GSSG, glutathione disulfide.

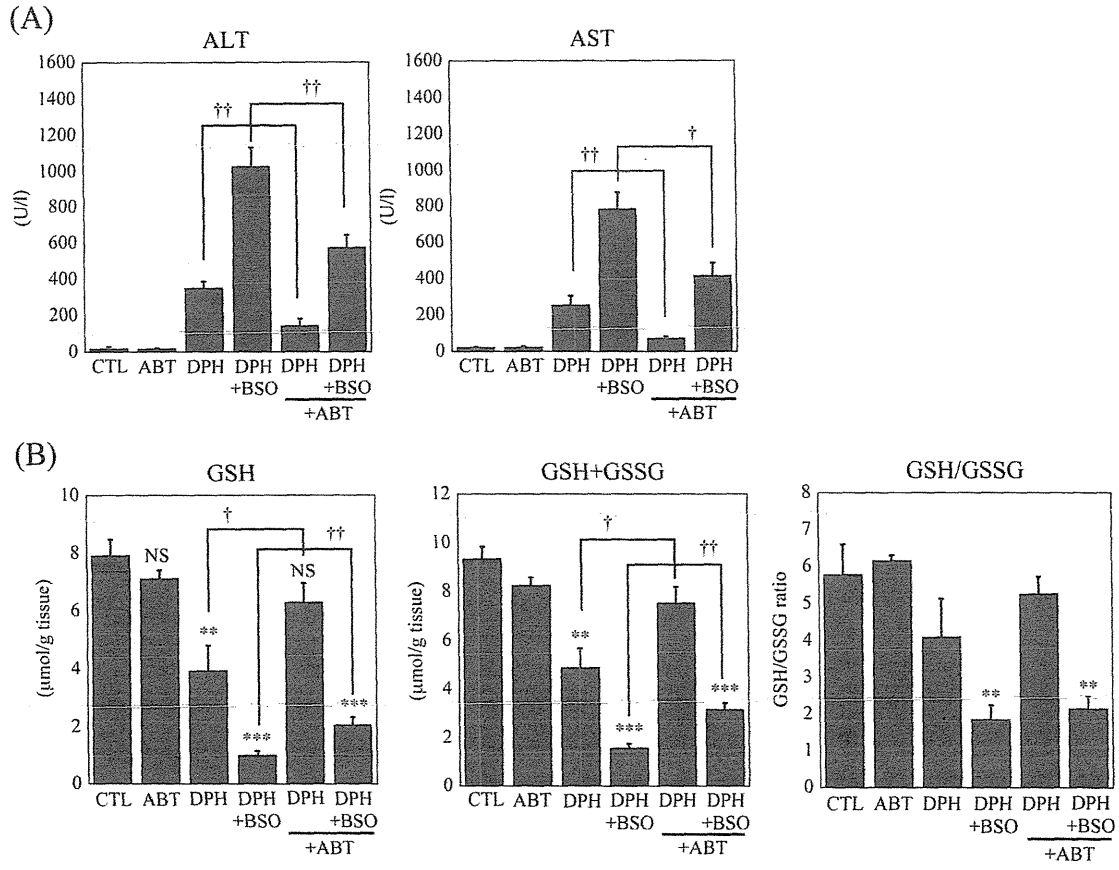

FIG. 3. Effect of a P450 inhibitor on plasma ALT and AST and hepatic GSH and GSSG levels in DPH-induced liver injury. The mice were IP given DPH at 50 mg/kg for 2 days, and then they were orally administered 100 mg/kg DPH on days 3 through 5. BSO was IP injected 1 h prior to each DPH treatment. ABT (100 mg/kg), a nonspecific inhibitor of P450, was IP given 1 h prior to the final DPH treatment. Each vehicle was used as a control. At 24 h after the final DPH treatment, the liver and plasma were collected to measure plasma ALT and AST levels (A), hepatic GSH and GSH + GSSG levels, and the GSH/GSSG ratio (B). The data are shown as the mean ± SEM of the results from 4 mice. The differences relative to the control mice were considered significant at $*p < .05$, $**p < .01$, and $*** p < .001$, and the differences between the ABT-treated and vehicle-treated mice were considered significant at $\dagger p < .05$, $\dagger\dagger p < .01$. Abbreviations: ABT, 1-aminobenzotriazole; ALT, alanine aminotransferase; AST, aspartate aminotransferase; DPH, 5,5-diphenylhydantoin; GSH, glutathione; GSSG, glutathione disulfide; NS, not significant.

at 1.5 h, and the expression level of S100A9 was significantly increased at 12 h after the final DPH treatment. To investigate whether HMGB1 is involved in the onset of inflammation, the plasma concentration of the HMGB1 protein was measured. HMGB1 is secreted from activated immune cells and is also released from necrotic cells. Therefore, we measured plasma HMGB1 protein levels using an ELISA and observed that they were significantly increased 3 h after the final DPH treatment in mice given both DPH and BSO (Fig. 4B). These results suggest that DAMPs are involved in the onset of inflammation.

To investigate whether TLR4 signaling and HMGB1 are involved in DPH-induced liver injury, eritoran, a specific TLR4 antagonist, or an anti-HMGB1 antibody was used. Treatment with either eritoran or the anti-HMGB1 antibody significantly suppressed the elevation of plasma ALT levels, suggesting that HMGB1 and TLR4 signaling may be involved in DPH-induced liver injury (Figs. 4C and D).

Changes in the Expression Levels of NALP3 Inflammasome-Related Factors

To investigate whether the NALP3 inflammasome is involved in the onset of inflammation, time-dependent changes in the hepatic mRNA expression levels of NALP3 and IL-1β were measured (Fig. 5A). The mRNA expression levels of IL-1β and NALP3 were significantly increased 1.5 h after the final DPH treatment. We then investigated whether the plasma concentration of the IL-1β protein is related to the onset of inflammation. The plasma IL-1β protein level was significantly increased 3 h after the final DPH treatment (Fig. 5B). These results suggest that NALP3 inflammasome activation leading to IL-1β production is involved in the onset of inflammation.

Changes in the Expression Levels of Th Cell-Related Transcription Factors, Cytokines, and Chemokines

To investigate whether inflammatory factors are involved in DPH-induced liver injury, we measured the time-dependent